NATIONAL ADVISORY COMMITTEE FOR AERONAUTICS

TECHNICAL NOTE 4228

EFFECTS OF FIXING BOUNDARY-LAYER TRANSITION FOR AN UNSWEPT-WING MODEL AND AN EVALUATION OF POROUS TUNNEL-WALL INTERFERENCE FOR MACH NUMBERS FROM 0.60 TO 1.40

By Louis S. Stivers, Jr., and Garth W. Lippmann

Ames Aeronautical Laboratory
Moffett Field, Calif.

Washington
April 1958

NATIONAL ADVISORY COMMITTEE FOR AERONAUTICS

TECHNICAL NOTE 4228

EFFECTS OF FIXING BOUNDARY-LAYER TRANSITION FOR AN UNSWEPT-WING MODEL AND AN EVALUATION OF POROUS TUNNEL-WALL INTERFERENCE FOR MACH NUMBERS FROM 0.60 TO 1.40

By Louis S. Stivers, Jr., and Garth W. Lippmann

SUMMARY

An investigation has been made in the Ames 2- by 2-foot transonic wind tunnel to determine the aerodynamic effects of fixing boundary-layer transition in a forward location on two unswept-wing models differing only in size and having unswept wings of aspect ratio 3.09 with sharp leading edges. The tests were made at Mach numbers from 0.60 to 1.40 and at Reynolds numbers from 1.5 to 3.45 million.

The effects of fixing transition were very pronounced on the pitching-moment and lift curve slopes at transonic Mach numbers, but were small at Mach numbers above about 1.15. For the fixed-transition condition the variations with Mach number of the pitching-moment and lift curve slopes were much smoother than for the free-transition condition. Within the range of the test Reynolds numbers the effects of fixing transition remained qualitatively the same. The results indicate that for tests at transonic Mach numbers of scale models with unswept wings, it is important to fix transition at locations corresponding to those expected in flight.

An evaluation of the interference of the porous walls in the Ames 2- by 2-foot transonic wind tunnel was made utilizing the fixed-transition data for the different-sized models. The evaluation indicated that the wall interference was generally small for the largest model employed in the investigation. This model had a projected frontal area of 1.2 percent of the cross-sectional area of the wind-tunnel test section. The limiting value of 0.5 percent indicated in the preliminary evaluation of porous-wall interference for these models, reported in NACA RM A55I21, is incorrect. In the selection of model size for small interference due to porous tunnel walls, the present results afford a guide only for models geometrically similar to the wing-body model of the present investigation. In general, the selection depends on factors in addition to the projected frontal area relative to the tunnel cross-sectional area.

INTRODUCTION

Aerodynamic characteristics of full-scale aircraft are generally deduced from small-scale model tests at Reynolds numbers much lower than those corresponding to flight. This procedure has merit, however, only when the model data can be reliably extended to full-scale conditions. The usually low test Reynolds numbers can be a source of difficulty, especially at the lower incidences where more extensive regions of laminar boundary layer are likely to exist on the model than on the aircraft. Whenever the boundary-layer characteristics on the model over a range of incidences and Mach numbers are substantially different from those on the aircraft, there is always the possibility that the distributions of pressures on the model will not correspond to those on the aircraft. This can be the case particularly at transonic Mach numbers because of the various effects of shock-wave boundary-layer interactions resulting from different boundary-layer conditions. The difficulty is not only that the effects may be large, but also that the effects are unpredictable.

The results of shock-wave boundary-layer investigations, such as those reported in reference 1, indicate that the Reynolds number effects are substantially reduced if the boundary layer ahead of the shock waves is turbulent. This would suggest that for a case when comparatively small regions of laminar boundary layer are expected on the aircraft and relatively extensive regions are found on the scale model, transition should be fixed at a forward position on the model to correspond more nearly to that on the aircraft in flight. Accordingly, the difficulties associated with the application of the small-scale test results to the aircraft may be expected to be minimized. The data of references 2 and 3 have shown that when transition is fixed on the forward portion of a model, the resulting aerodynamic characteristics can be appreciably different from those measured when transition is left free and occurs relatively far rearward. Also reported in references 2 and 3 are summaries of numerous tests in which the problems associated with fixing transition, such as the device to be used and its size, were investigated.

Of the known published high-speed aerodynamic data showing the effects of fixing transition, only a small amount corresponds to three-dimensional configurations. Further research is needed, particularly at transonic Mach numbers, to determine the combined effects of fixing transition and of Reynolds number on the aerodynamic characteristics of models having wings of various plan forms. Some information of this type has recently been obtained in an extensive investigation in the Ames 2- by 2-foot transonic wind tunnel of a model having an unswept wing with a sharp leading edge and having transition fixed at a forward location. The present report summarizes the results of the investigation.

Also included in this report is an evaluation of the effects of porous-wall interference in the Ames 2- by 2-foot transonic wind tunnel on the aerodynamic characteristics of the unswept-wing configuration with transition fixed. A preliminary evaluation of the wall effects of this wind tunnel employing the same models with transition free has been reported in reference 4.

NOTATION

C_D drag coefficient

C_L lift coefficient

C_{L_α} lift curve slope, $\frac{\partial C_L}{\partial \alpha}$

C_m pitching-moment coefficient referred to $\bar{c}/4$ (see fig. 1)

$C_{m_{C_L}}$ pitching-moment curve slope, $\frac{\partial C_m}{\partial C_L}$

c local chord of wing

c_t local chord of horizontal tail

$\bar{c}$ mean aerodynamic chord of wing

$\bar{c}_t$ mean aerodynamic chord of horizontal tail

M free-stream Mach number

R Reynolds number

α angle of attack, deg

APPARATUS AND TESTS

Models

Two geometrically similar models of different size were employed in the present investigation. These were the "medium" and "large" models which had been employed in the preliminary investigation of wall effects reported in reference 4. For consistency, the models will also be designated "medium" and "large" in the present report. The magnitudes of the blockage of these models in the Ames 2- by 2-foot tunnel are 0.5 and 1.2 percent. (Model blockage, in percent, is defined as 100 times the ratio of projected frontal area of the model to the cross-sectional area of the wind-tunnel test section.) The linear dimensions of the large model are 1.5 times the corresponding dimensions of the medium model. The configuration of the medium model is shown in figure 1 together with other geometric information. The tail unit was available only for the medium model. Each model was constructed of steel. The wing and horizontal-tail panels had sharp leading edges and were fixed on the body at zero incidence with no dihedral. The vertical tail employed the NACA 0003 airfoil section in the streamwise direction.

Transition was fixed on the models by means of a 0.005-inch-diameter wire which was attached to the model surfaces by means of clear lacquer. A transition-wire ring on the body was located at a station 1-1/3 inches from the apex of the body nose on the medium model, and 2 inches from the apex on the large model. On the wing and horizontal-tail surfaces, the transition wires were located along rays from the leading-edge apex to the quarter-chord point of the tips. Transition was not fixed on the vertical tail.

Wind Tunnel and Model Support

The investigation was conducted in the Ames 2- by 2-foot transonic wind tunnel. This wind tunnel utilizes a flexible nozzle and porous test-section walls to permit continuous operation to a Mach number as high as 1.4, and to provide choke-free flow in the test section throughout the transonic Mach number range. A given Reynolds number can be maintained throughout the operational range of Mach numbers by varying the stagnation pressure within the wind tunnel. A detailed description of the tunnel is given in reference 4.

For the tests the models were mounted on sting-supported, flexure-type balances which were enclosed within the bodies of the models. The ratios of model base diameter to sting diameter for the medium and large models were identical. Electrical-resistance strain gages were employed to measure the forces and moments on the models.

Tests

Lift, drag, and pitching-moment data were obtained at 20 Mach numbers ranging from 0.60 to 1.40 and for angles of attack ranging from about -4° to 13°, except when either the loads on the balances or the power supplied to the tunnel drive motors reached limiting values. Each model was tested at two Reynolds numbers; the medium model at 1.5×10^{6} and 2.3×10^{6}, and the large model at 1.5×10^{6} and 3.45×10^{6} (Reynolds numbers based on wing mean aerodynamic chord). The largest Mach number attainable at the higher Reynolds numbers was 1.20. The measurements were made with the models in the free- and fixed-transition conditions. The visualization technique described in reference 5 was used in brief tests to determine the effectiveness of the wires in producing transition.

CORRECTIONS AND PRECISION

No corrections for the effects of the test-section walls have been applied to the data of this report. A preliminary evaluation of such effects reported in reference 4 (boundary-layer transition free) has shown that the magnitudes of the corrections for the medium-model data are small, for the most part. Furthermore, the examination of wall-interference effects made later in this report (boundary-layer transition fixed) has indicated that the magnitudes of the corrections for the large-model data are essentially the same as those for the medium-model data.

Other factors which could have influenced the measured data have been considered and have been dealt with in various ways. Stream-angularity corrections were found to be insignificant and are not included. The axial forces measured by the internal balance have been adjusted to correspond to a condition of free-stream static pressure at the base of the body.

The transition-fixed drag data have not been corrected for the contribution due to the wires. The increment in drag coefficient due to the transition wires could not be accurately determined from the data of the present investigation. It was estimated, however, that for transition wires on the body nose and on both surfaces of the wing and horizontal tail the increment varied from 0.0012 to 0.0015 over the test range of Mach numbers, and for wires only on the wing, from 0.0007 to 0.0009. For the estimations, the drag of the wires was assumed to result principally from pressure differences across the upstream and downstream sides of the wires. Pressure data measured on forward and rearward facing steps, which were obtained from reference 6 and from unpublished investigations in the Ames 1- by 3-foot and 1- by 3-1/2-foot wind tunnels, were employed in the calculations. Pressures were used that most nearly corresponded to the local boundary-layer conditions, ratio of wire diameter to length of boundary-layer run upstream of the wire, and local Reynolds and Mach numbers at the position of the transition wires on the model. (The boundary layer ahead of the wires was laminar and transition occurred at a distance behind the wires of the order of 10 wire diameters.) It was noted that the pressures on the steps varied substantially depending on whether the boundary layer was laminar, transitional, or turbulent. For low supersonic Mach numbers the pressure differences across the faces of a step simulating a wire were roughly twice as much for a turbulent boundary layer as for a laminar boundary layer. The present method of estimating the drag of the wires has been substantiated for the condition of a turbulent boundary layer over the wires. For this condition, increments in drag due to the wires were determined experimentally in the wind tunnel simply by adding a second wire on the wing parallel to and one-quarter-inch downstream of the initial transition wire. The experimental increment in drag due to the second wire varied from 0.0011 to 0.0022 over the Mach number range from 0.60 to 1.40, whereas the corresponding estimated increments varied from 0.0013 to 0.0018.

In addition to the small systematic errors which may be introduced by the corrections that have been neglected, the test data are subject to random errors of measurement that influence the precision of the measured data. The methods of reference 7 were used to evaluate the precision of Mach number, angle of attack, Reynolds number, and lift, drag, and pitching-moment coefficients for the data obtained using the medium model of the present investigation. The random uncertainties associated with the medium model are given in the following table for low and moderate angles of attack, and for three representative Mach numbers:

Item	M = 0.60		M = 1.00		M = 1.40	
	$\alpha = 0.25^\circ$	$\alpha = 6^\circ$	$\alpha = 0.25^\circ$	$\alpha = 6^\circ$	$\alpha = 0.25^\circ$	$\alpha = 6^\circ$
M	±0.002	±0.002	±0.002	±0.002	±0.002	±0.002
α	$\pm.02^\circ$	$\pm.01^\circ$	$\pm.02^\circ$	$\pm.03^\circ$	$\pm.02^\circ$	$\pm.02^\circ$
R	$\pm.03\times10^6$	$\pm.03\times10^6$	$\pm.02\times10^6$	$\pm.02\times10^6$	$\pm.08\times10^6$	$\pm.08\times10^6$
C_L	±.004	±.005	±.002	±.007	±.001	±.005
C_D	±.0002	±.0004	±.0002	±.0011	±.0002	±.0010
C_m	±.003	±.004	±.002	±.007	±.001	±.005

The random uncertainties of the lift, drag, and pitching-moment coefficients and angles of attack associated with the large model are believed to be no greater than those given above for the medium model. The uncertainties of Mach number and Reynolds number would be unaffected by the change in models.

RESULTS AND DISCUSSION

Examination of the results of the present investigation has indicated that the effects of fixing transition can be adequately summarized in a comparison of the values of pitching-moment curve slope, $C_{m_{C_L}}$, lift curve slope, C_{L_α}, and drag coefficient for the various conditions. Accordingly, most of the results are given in this form and are presented for lift coefficients of 0, 0.2, and 0.4 as functions of Mach number. Some basic data, however, are presented for a few selected Mach numbers to show the results for constant Mach number and varying incidence. The basic data are on file at the Ames Laboratory of the NACA and can be obtained upon request.

Effects of Fixing Transition

Reynolds number of 1.5 million.- Variations of the pitching-moment and lift curve slopes with Mach number as affected by fixing transition[1]

[1]Results of boundary-layer visualization tests throughout the Mach number range employing the diffusible-solid technique described in reference 5 indicated that the wires effectively caused transition some 10 wire diameters downstream of the wires at low angles of attack.

on the wing, body, and tail are shown in figures 2 and 3, respectively. (The corresponding data for the large model indicate essentially the same effects as the data for the medium model and are not shown for this reason.) Large effects of fixing transition are generally observed at subsonic and transonic Mach numbers, but only small effects are evident at Mach numbers above about 1.15. The abrupt changes in lift and pitching-moment curve slopes with variation in Mach number shown for the free-transition condition (such as for a Mach number of 0.95 at zero lift) are smoothed out considerably for the fixed-transition condition. This is especially true for the pitching-moment curve slopes. A full-scale airplane which has pitching-moment characteristics like those for the model with transition free would probably experience undesirable trim changes in regions corresponding to the marked changes in pitching-moment curve slopes. Since the location of transition on the airplane, however, is not likely to be relatively as far rearward as that on the scale model at low Reynolds number, it can be inferred that the transition-free data would provide misleading results if an attempt were made to extrapolate such data to full-scale conditions. Accordingly, the importance of fixing transition on scale models at locations corresponding to those expected in flight is readily apparent.

The variations of drag coefficient with Mach number are given in figure 4 for the tail-off configuration of the medium model. Large increments in drag coefficient due to fixing transition are evident in this figure. At zero lift, only about 20 percent of the increment is due to the drag of the wires, whereas the remaining 80 percent is due to the increase in skin friction. (The procedure for estimating the drag of the wires is briefly described in the "CORRECTIONS AND PRECISION" section of this report.) It is noted in figure 4 that the increments generally decrease with increasing lift coefficient, as would be expected. The effects of Reynolds number on the increments in drag coefficient due to fixing transition are discussed in the next section of this report.

Typical basic lift, drag, and pitching-moment data are presented in figure 5. (Reliable drag data are not available for the complete model in the transition-free condition.) It is apparent that the effects of fixing transition are the most pronounced for the pitching-moment and drag data. Substantial effects are observed for lift coefficients as high as about 0.7 for a Mach number of 0.94.

<u>Reynolds numbers of 2.3 and 3.45 million</u>.- In an effort to provide some indication of the influence of Reynolds number on the effects of fixing transition, the tail-off configuration of the medium and large models was tested at Reynolds numbers of 2.3 and 3.45 million, respectively. The effects of Mach number on the pitching-moment and lift curve slopes are shown in figures 6 and 7, respectively, for the two models at these Reynolds numbers. Data were unobtainable for a Reynolds number of 3.45 million at a lift coefficient of 0.4 for Mach numbers from about 0.94 to 1.06 and above a Mach number of about 1.12. The variations of drag coefficient with Mach number for the models are given in figure 8.

Typical basic lift, drag, and pitching-moment coefficients for the two models are shown in figure 9 for a Mach number of 0.94. For comparison in figures 6 to 9, the corresponding data for a Reynolds number of 1.5 million with transition fixed on the models are also presented.

It is observed in figures 6 to 9 that the effects of fixing transition at Reynolds numbers of 2.3 and 3.45 million are also significant and are qualitatively the same as those for a Reynolds number of 1.5 million. It should be noted that the fixed-transition data for the higher Reynolds numbers are generally in good agreement with the corresponding fixed-transition data for a Reynolds number of 1.5 million, except for the expected differences in the level of the drag coefficients resulting from the differences in Reynolds number.

Additional information concerning the effects of Reynolds number on the magnitude of the minimum drag coefficients is given in figure 10, where measured values of drag coefficient at zero lift for a Mach number of 0.60 are presented for the fixed- and free-transition conditions at Reynolds numbers varying from about 1.0 to 3.45 million. Also shown in this figure are calculated curves for the models with fully turbulent and fully laminar boundary layers. The calculations were made using the wetted areas of the wing and body, and flat-plate skin-friction coefficients which for the turbulent boundary layer were determined from reference 8 and were corrected to a Mach number of 0.60 by the data of reference 9. For the laminar boundary layer the skin-friction coefficients were obtained from the expression $1.328\ R^{-1/2}$. It is evident in figure 10 that the measured drag coefficients for the fixed-transition condition are very closely approximated by the corresponding calculated values. The agreement in the trends of the two curves is remarkable. For the transition-free case, the measured drag coefficient at a Reynolds number of 1.0 million is about double the value calculated for a fully laminar boundary layer. As the Reynolds number is increased, the measured values depart more from the calculated laminar curve and approach the calculated turbulent curve, indicating an average forward movement of free transition on the model for a Mach number of 0.60. The zero-lift drag data of figures 4 and 8 indicate that this forward movement was not appreciably affected by Mach number.

Wall Effects in the Ames 2- by 2-Foot Transonic Wind Tunnel for an Unswept-Wing-Body Model

It has been shown by the data already presented that the pitching-moment and lift curve slopes of the unswept-wing models with boundary-layer transition fixed in a forward location are materially different at transonic Mach numbers from those slopes corresponding to the free-transition condition. In addition, it has been noted that the slopes corresponding to the fixed-transition condition vary much more smoothly with Mach number. Inasmuch as the evaluation of porous-wall interference from transition-free data reported in reference 4 may have been influenced by differences in boundary-layer conditions on the models employed during the tests, it was believed that a re-evaluation of the effects should be made using the present fixed-transition data.

To evaluate the wall-interference effects the fixed-transition 1.5-million Reynolds number data for the tail-off configuration of the medium and large models are compared with unpublished fixed-transition data from tests of the large model at a Reynolds number of approximately 1.5 million in the Ames 6- by 6-foot supersonic wind tunnel. The same large model and balance used in the present investigation were employed in the Ames 6- by 6-foot wind-tunnel tests. The magnitudes of the blockages of the medium and large models in the Ames 2- by 2-foot tunnel are 0.5 and 1.2 percent, respectively, and that of the large model in the Ames 6- by 6-foot tunnel is 0.1 percent.

The variations of pitching-moment and lift curve slopes with Mach number for the different amounts of model blockage are shown in figures 11 and 12, respectively. It is immediately apparent in these figures that the values of the slopes for the three blockages are in good agreement, with minor exceptions. The differences, in general, are less than those shown earlier in this report between the fixed- and free-transition data for a given model. It is of particular significance to observe that the 0.5- and 1.2-percent-blockage data are in about equal agreement with the 0.1-percent data, indicating that within the accuracy of the data the wall interference is essentially the same for these two blockages. Irregularities are evident in the 0.5- and 1.2-percent-blockage data at the low-supersonic Mach numbers, which introduce significant differences in the magnitudes of the slopes for these two blockages. Such irregularities are apparently due to wave reflections from the walls of the test section. Note particularly that the 0.1-percent-blockage data would lie very near a smooth curve faired through the irregularities in the data for the higher blockages. That such a faired curve represents interference-free data very well appears to be substantiated by preliminary unpublished data for the large model tested in the Ames 14-foot tunnel (model blockage of 0.03 percent). These tests were made for increments in Mach numbers of 0.02 between Mach numbers of 0.90 and 1.10.

The variations of drag coefficient with Mach number for the several amounts of model blockage are presented in figure 13 for lift coefficients of 0, 0.2, and 0.4. For zero lift coefficient, there is little effect of change in blockage. A slight decrease in drag coefficient with an increase in blockage, however, is apparent for Mach numbers from about 1.0 to 1.1. At successively higher lift coefficients it is observed that the differences in the drag coefficients for the three blockages become, in general, progressively greater. The reasons for these greater differences are not known. The differences for Mach numbers above about 0.95, however, are probably not indicative of the wall-interference effects since the agreement between the 0.5- and 1.2-percent-blockage data is generally good at these Mach numbers.

The lift, drag, and pitching-moment characteristics of the tail-off configuration with fixed transition are shown for the various model blockages in figure 14 at constant Mach numbers. The agreement among these data is generally good, thus indicating that, on the whole, the effects of wall interference are not substantially different for the magnitudes of model blockage employed in the present evaluation.

In the previous analysis of wall interference in the Ames 2- by 2-foot transonic wind tunnel (transition-free data) reported in reference 4, it was concluded that the largest size model for which reliable data could be obtained was one having 0.5-percent blockage. Although the lift, drag, and pitching-moment coefficients at constant incidence for the 1.2-percent-blockage model (ref. 4) compared favorably in some respects with the corresponding data for the 0.5-percent-blockage model, serious discrepancies in these characteristics were evident mainly in the supersonic Mach number range between 1.05 and 1.20. Since no serious discrepancies were indicated by the transition-fixed data of the present report, an effort was made to determine the reasons for the disagreement. An examination of the differences between the lift, drag, and pitching-moment coefficients at constant angles of incidence from the data of reference 4 and from the present investigation indicated that the previously mentioned discrepancies did not exist in the present data even for the transition-free condition. In general, fixing the transition proved to have only minor effects on the differences between the measured force and moment coefficients for the 1.2- and 0.5-percent-blockage models. The discrepancies noted in the data of reference 4 for these models appeared to have resulted from difficulties in accurately measuring the forces and moments on the models, particularly for the higher incidences. For the present tests, more accurate balances and equipment for recording the outputs of the balance strain gages were employed than were available for the investigation of reference 4. Inasmuch as the present data have indicated that the wall-interference effects appear to be generally small for an unswept-wing-body model having a blockage as large as 1.2 percent, it is apparent that the limit of 0.5 percent stated in reference 4 is incorrect.

CONCLUDING REMARKS

The results of the investigation to determine the aerodynamic effects of fixing transition at a forward location on the unswept-wing models for Reynolds numbers ranging from 1.5 million to 3.45 million indicated that fixing transition effected large changes in the pitching-moment and lift curve slopes at transonic Mach numbers, but produced only small changes at Mach numbers above about 1.15. The variations of the pitching-moment and lift curve slopes with Mach number were much smoother throughout the transonic Mach number range when transition was fixed than when left free. The effects of fixing transition were qualitatively unchanged within the range of the test Reynolds numbers. It has been noted that extrapolation of the transition-free data to full-scale conditions could provide misleading results in the transonic Mach number range. As a result, whenever tests are to be made within this range, it is important that transition be fixed on scale models at locations corresponding to those expected in flight.

The evaluation of porous-wall interference in the Ames 2- by 2-foot transonic wind tunnel, employing fixed-transition data obtained from tests of different sized models, indicated that the interference is generally small for an unswept-wing-body model having a projected frontal area as large as 1.2 percent of the cross-sectional area of the wind-tunnel test section. Inasmuch as the present data were obtained using more accurate equipment than was available for the preliminary investigation reported in NACA RM A55I21, the limiting value of 0.5 percent noted therein is evidently incorrect. In selecting the size of a model for small interference in a given porous-wall transonic wind tunnel, the present results are strictly applicable only when the model is geometrically similar to that of the present investigation. In general, the selection depends on factors in addition to the projected frontal area relative to the tunnel cross-sectional area. Such factors include the tail length or body length relative to the tunnel height (ref. 10).

Ames Aeronautical Laboratory
National Advisory Committee for Aeronautics
Moffett Field, Calif., Feb. 7, 1958

REFERENCES

1. Holder, D. W., Pearcey, H. H., and Gadd, G. E.: The Interaction Between Shock Waves and Boundary Layers. British A.R.C. Tech. Rep. C.P. No. 180, 1955. (Also available as I.A.S. Preprint 550)

2. Haines, A. B., Holder, D. W., and Pearcey, H. H.: Scale Effects at High Subsonic and Transonic Speeds, and Methods for Fixing Boundary-Layer Transition in Model Experiments. R.A.E. TN No. Aero. 2338, British, Sept. 1954.

3. Winter, K. G., Scott-Wilson, J. B., and Davies, F. V.: Methods of Determination and of Fixing Boundary-Layer Transition on Wind Tunnel Models at Supersonic Speeds. A.R.C. C.P. No. 212, British, Sept. 1954. (Also available as AGARD Rep. AG 17/p7, Nov. 1954)

4. Spiegel, Joseph M., and Lawrence, Leslie F.: A Description of the Ames 2- by 2-Foot Transonic Wind Tunnel and Preliminary Evaluation of Wall Interference. NACA RM A55I21, 1956.

5. Main-Smith, J. D.: Chemical Solids as Diffusible Coating Films for Visual Indications of Boundary-Layer Transition in Air and Water. R. & M. No. 2755, British, 1950.

6. Chapman, Dean R., Kuehn, Donald M., and Larson, Howard K.: Investigation of Separated Flows in Supersonic and Subsonic Streams With Emphasis on the Effect of Transition. NACA TN 3869, 1957.

7. Beers, Yardley: Introduction to the Theory of Error. Addison-Wesley Publishing Co., Cambridge, Mass., 1953.

8. Locke, F. W. S., Jr.: Recommended Definition of Turbulent Friction in Incompressible Fluids. NAVAER DR Rep. No. 1415, June 1952.

9. Chapman, Dean R., and Kester, Robert H.: Turbulent Boundary-Layer and Skin-Friction Measurements in Axial Flow Along Cylinders at Mach Numbers Between 0.5 and 3.6. NACA TN 3097, 1954.

10. Page, William A.: Experimental Study of the Equivalence of Transonic Flow About Slender Cone-Cylinders of Circular and Elliptic Cross Section. NACA TN 4233, 1958.

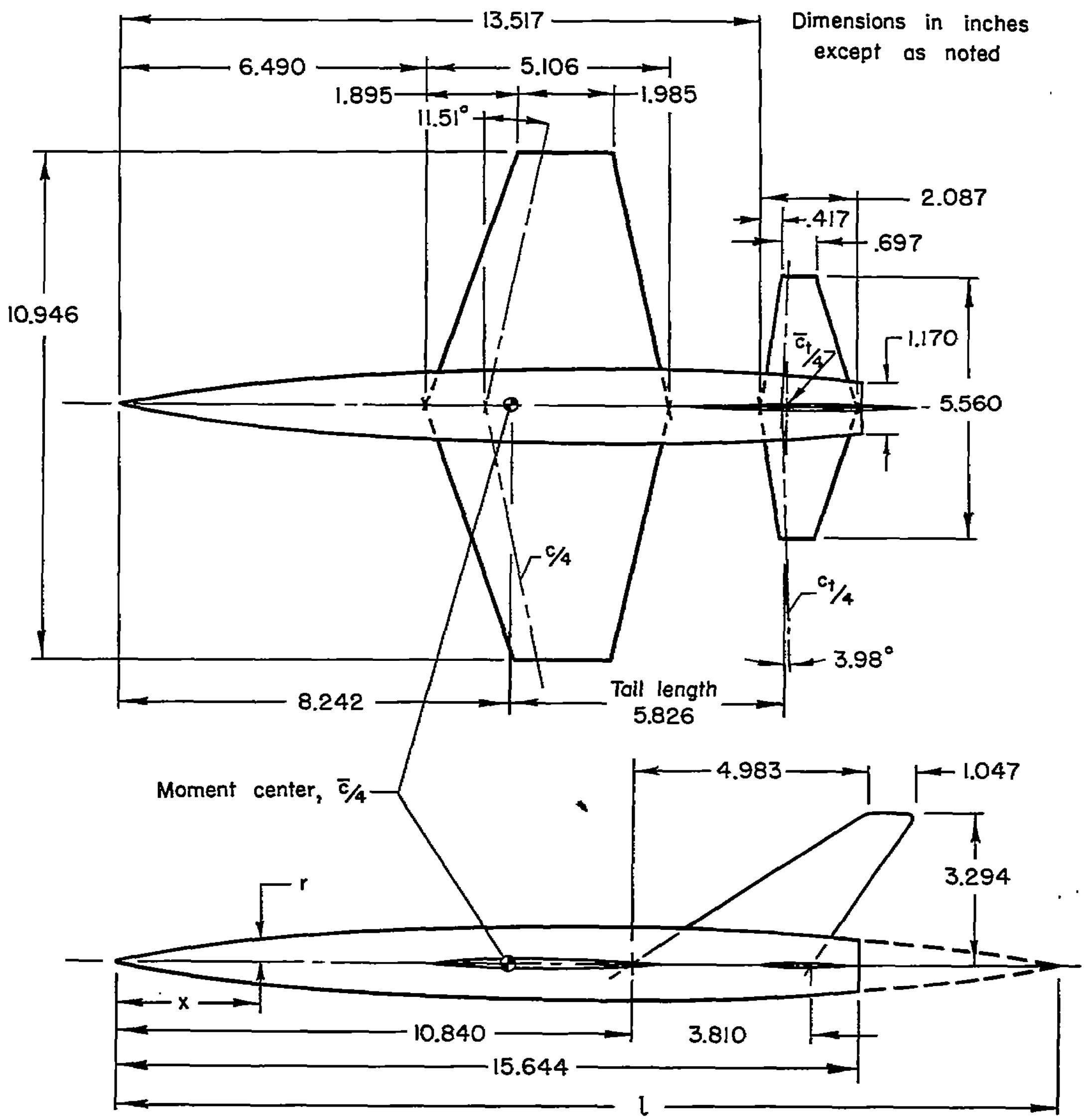

	Wing	Horizontal tail
Aspect ratio	3.09	3.99
Taper ratio	.39	.33
Thickness-chord ratio	.03	.03
Airfoil section	Biconvex	Circular arc (max. thickness at 0.3 chord)
Area	38.81 sq in.	7.74 sq in.
Mean aerodynamic chord	3.77 in.	1.51 in.
Location of unswept line	.61 c	.30 c_t

Body

Ordinates given by:

$$\frac{r}{r_o} = \left[1 - \left(1 - \frac{2x}{l}\right)^2\right]^{\frac{3}{4}}$$

Where:

r = local radius

$r_o = r_{maximum} = 0.794$

x = longitudinal distance from nose

$l = 2(x_{for\ r_o}) = 19.833$

Figure 1.- Geometrical information for the medium model.

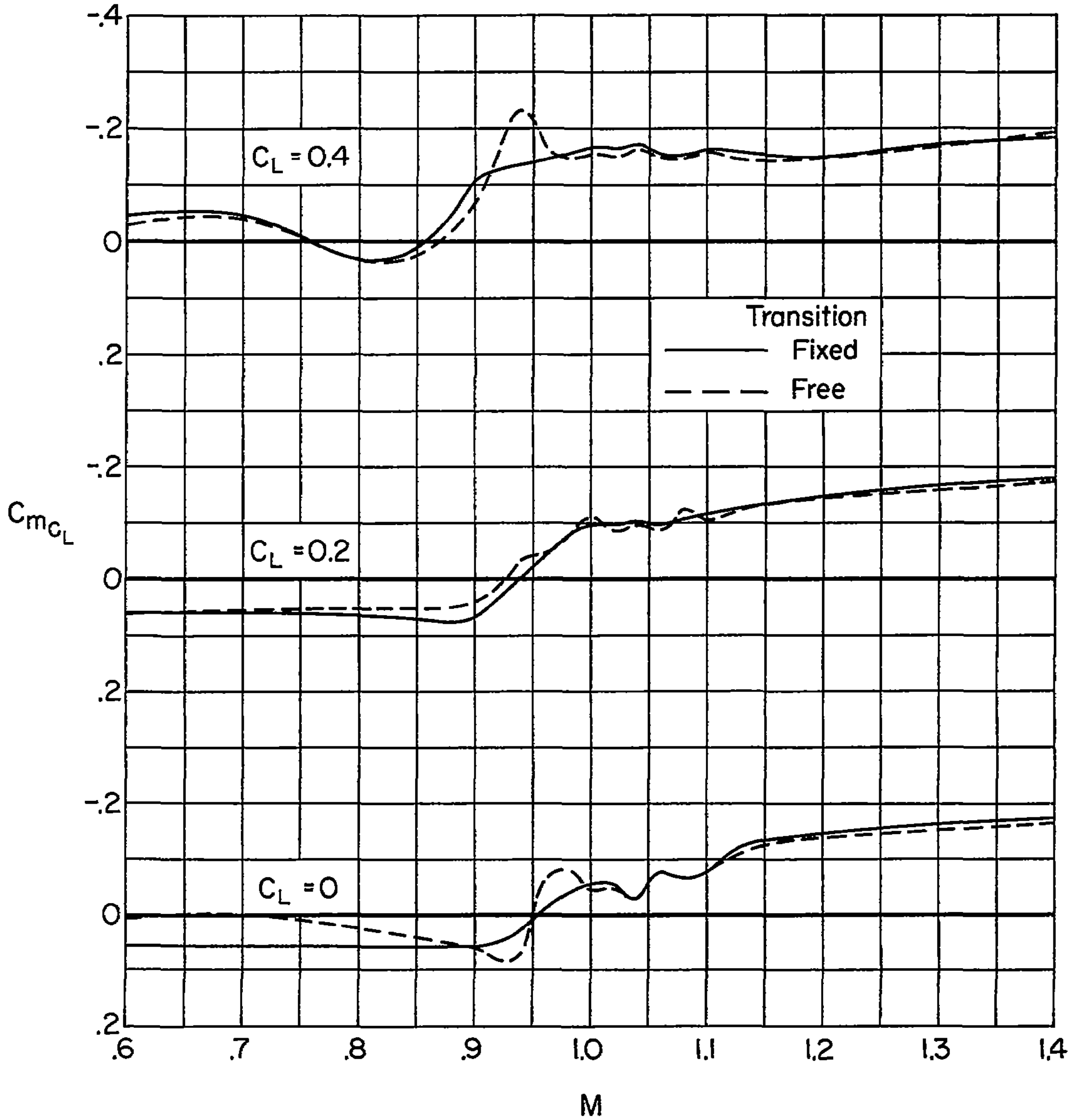

(a) Tail off.

Figure 2.- Variations of pitching-moment curve slope with Mach number as affected by fixing transition; R = 1.5×10^6, medium model.

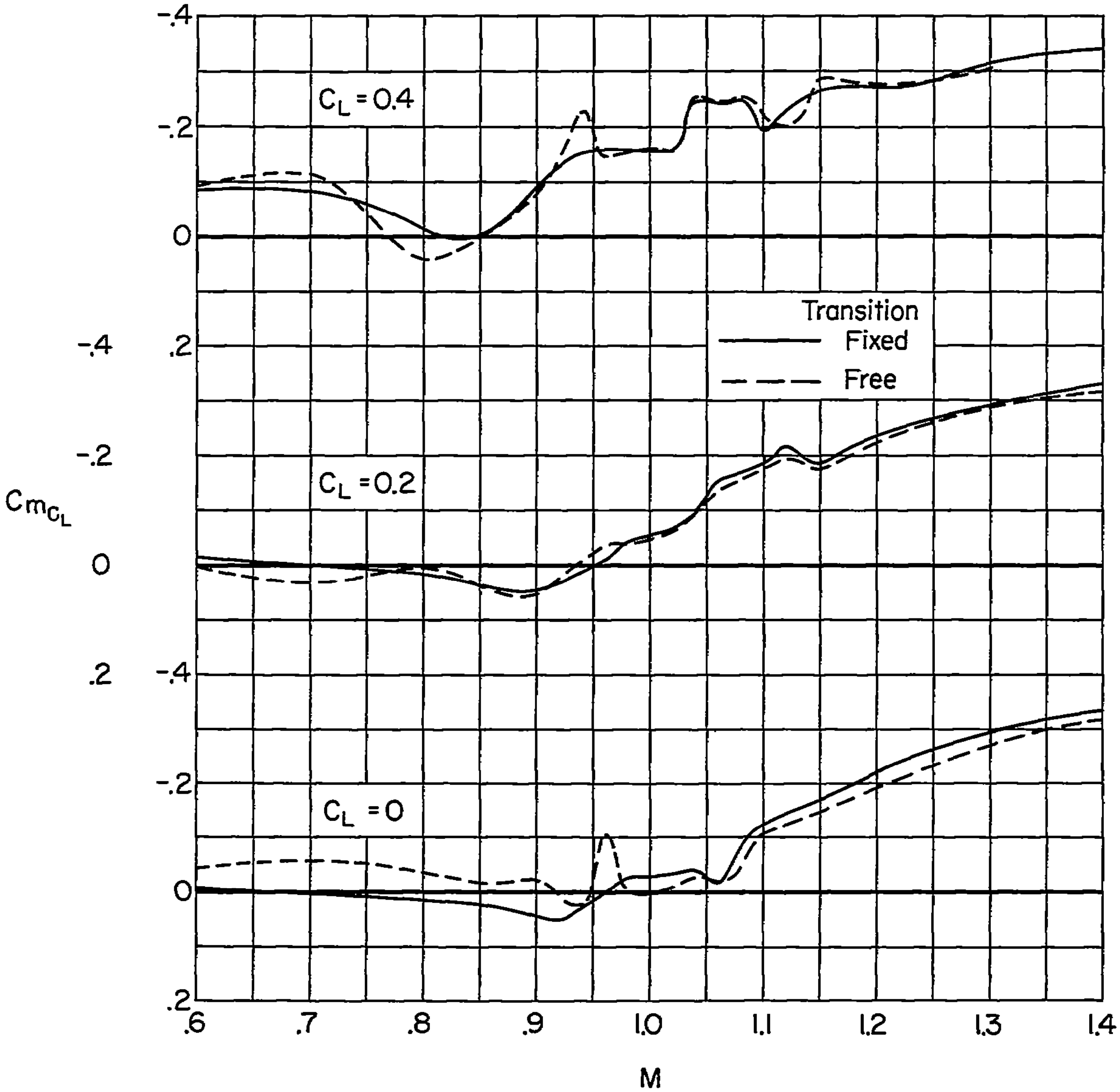

(b) Tail on.

Figure 2.- Concluded.

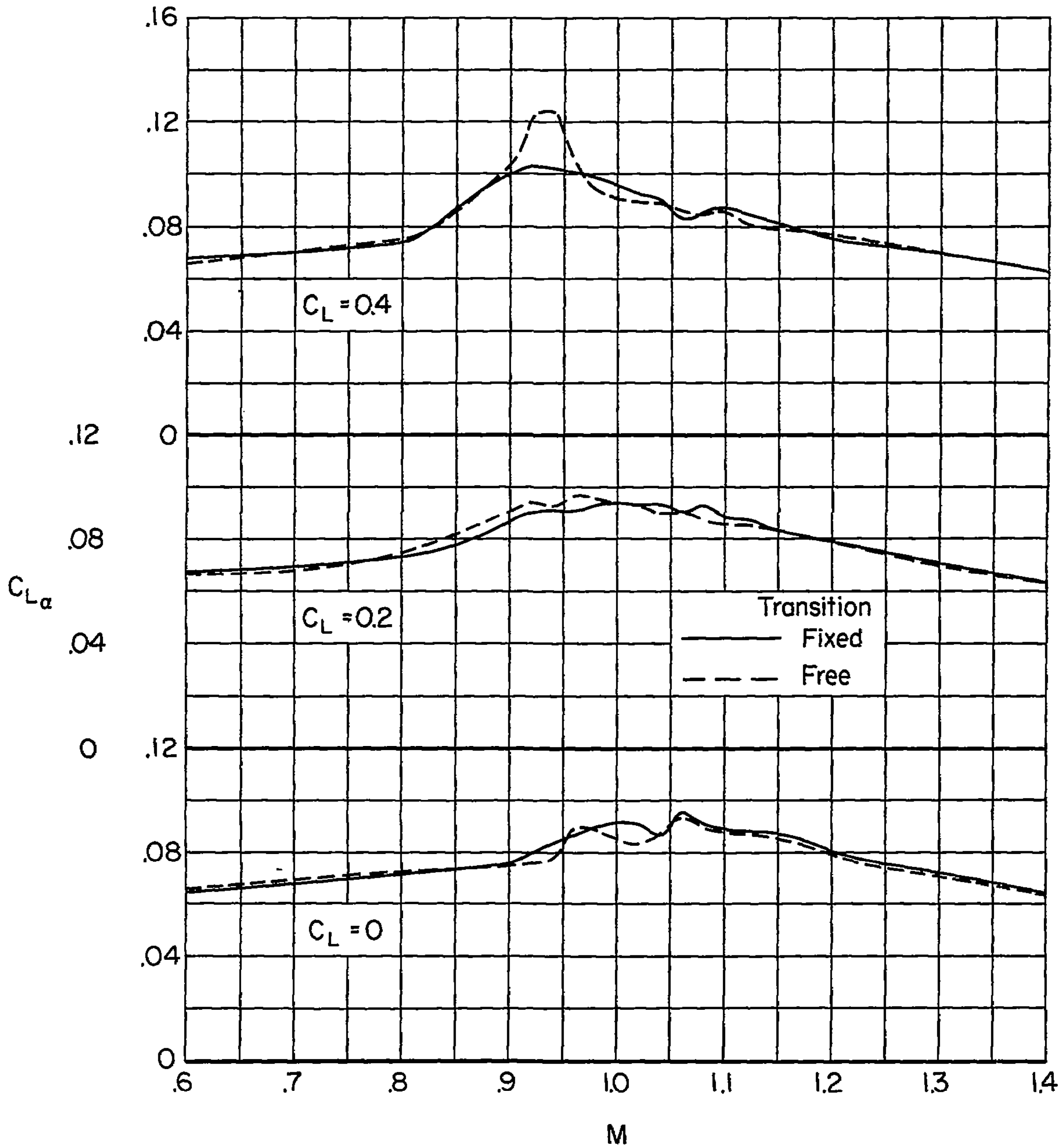

(a) Tail off.

Figure 3.- Variations of lift curve slope with Mach number as affected by fixing transition; $R = 1.5 \times 10^6$, medium model.

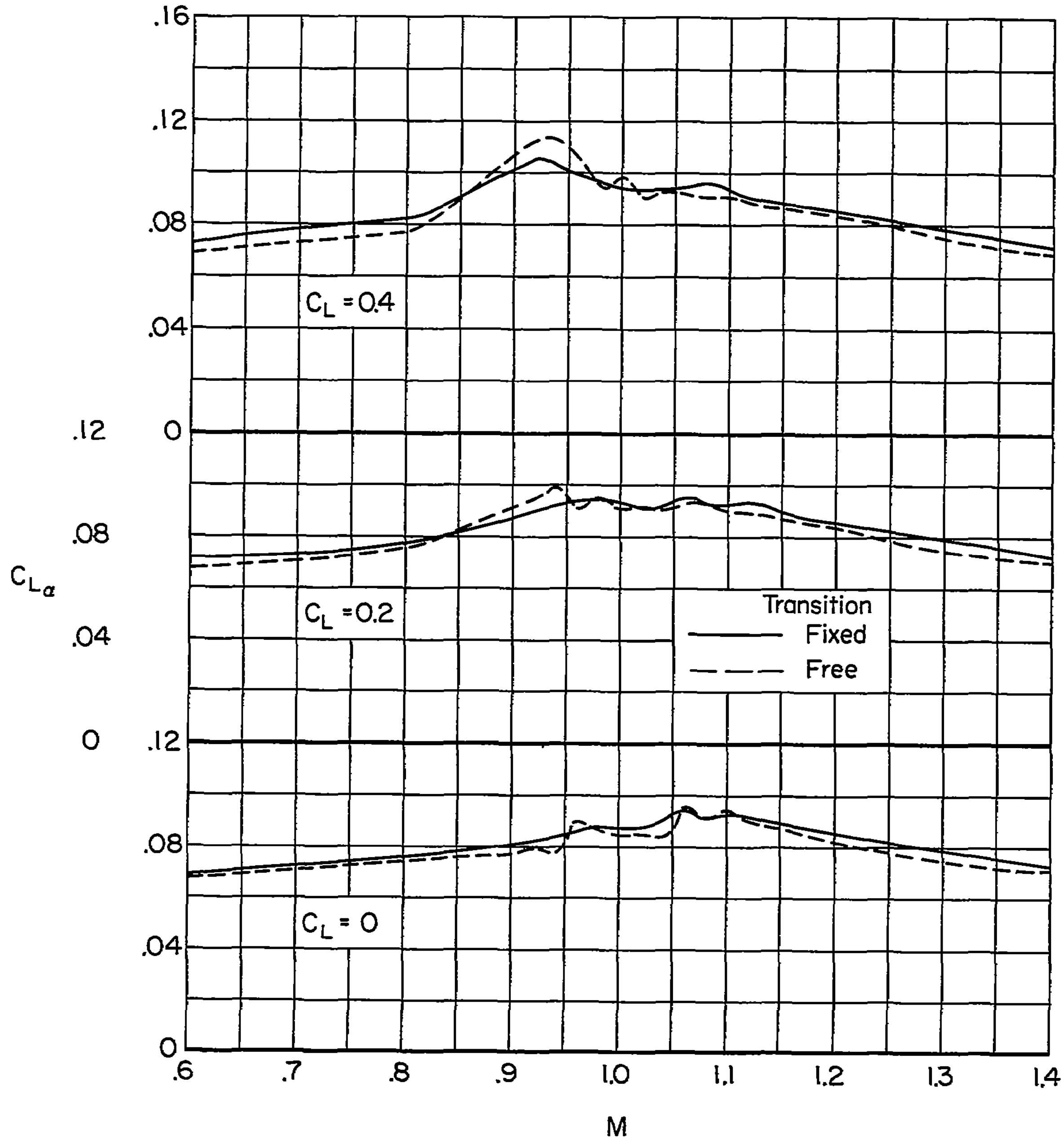

(b) Tail on.

Figure 3.- Concluded.

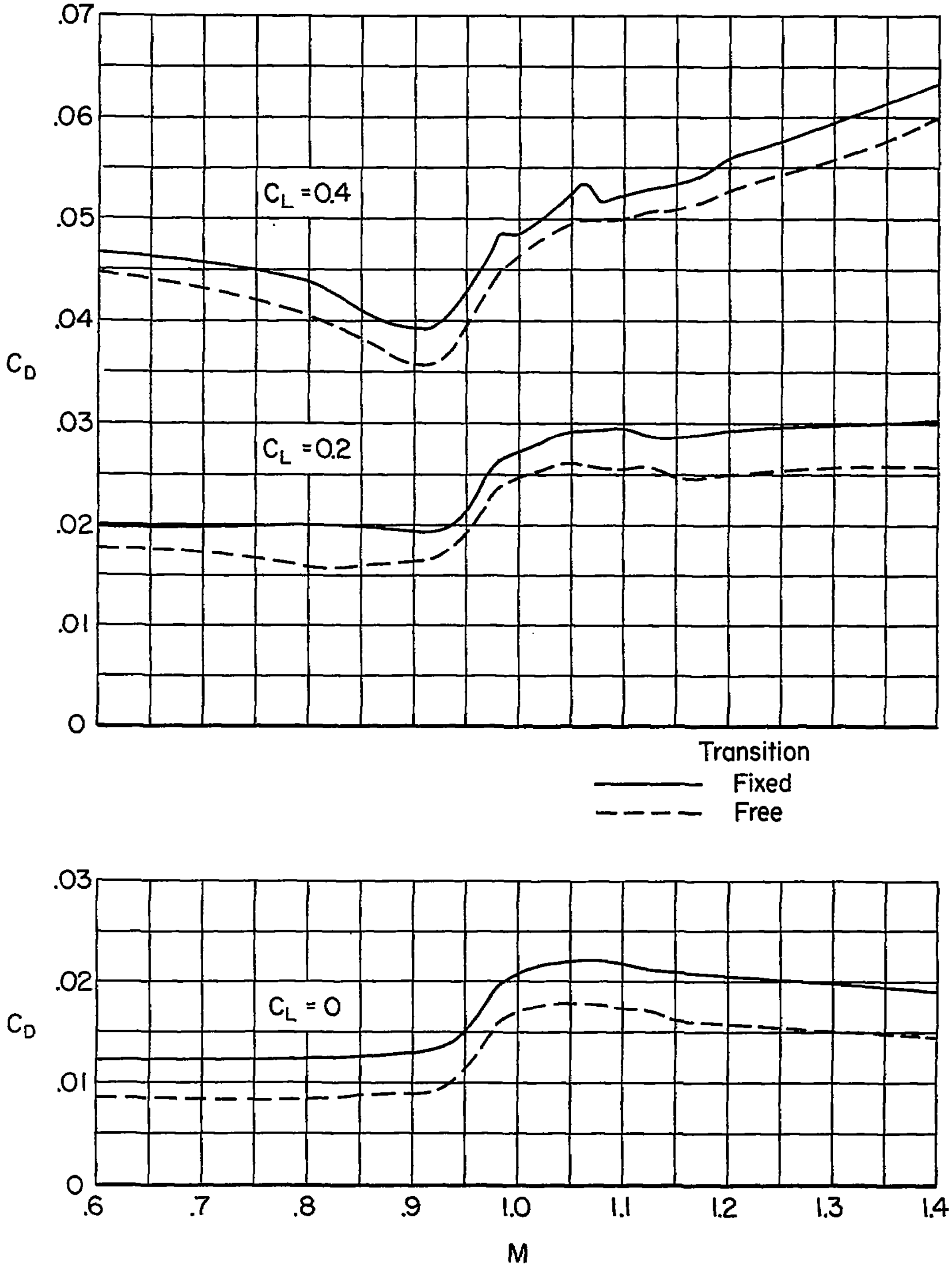

Figure 4.- Variations of drag coefficient with Mach number as affected by fixing transition; $R = 1.5 \times 10^6$, medium model, tail off.

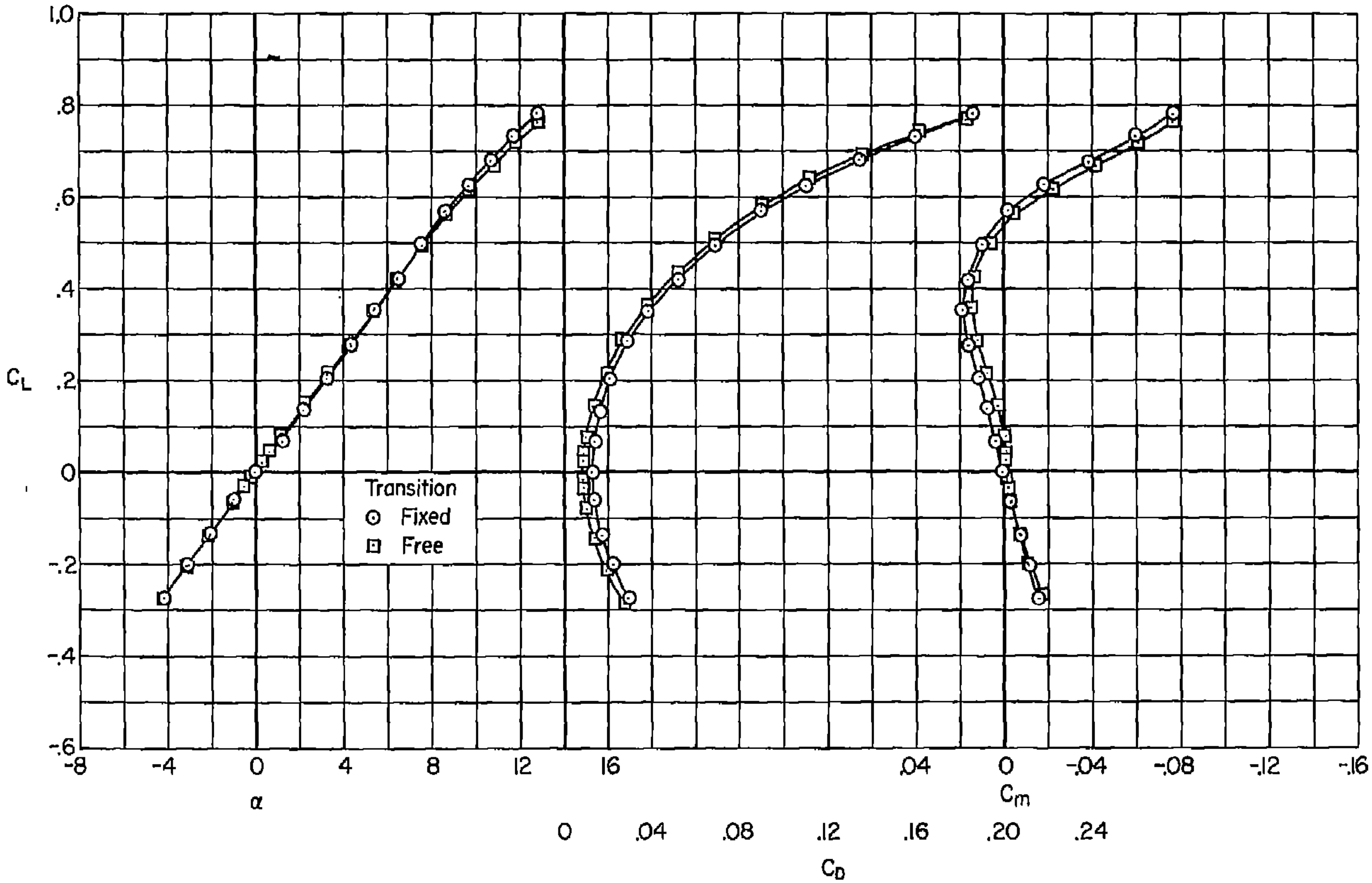

(a) Tail off, M = 0.60.

Figure 5.- Lift, drag, and pitching-moment characteristics as affected by fixing transition; R = 1.5×10[6], medium model.

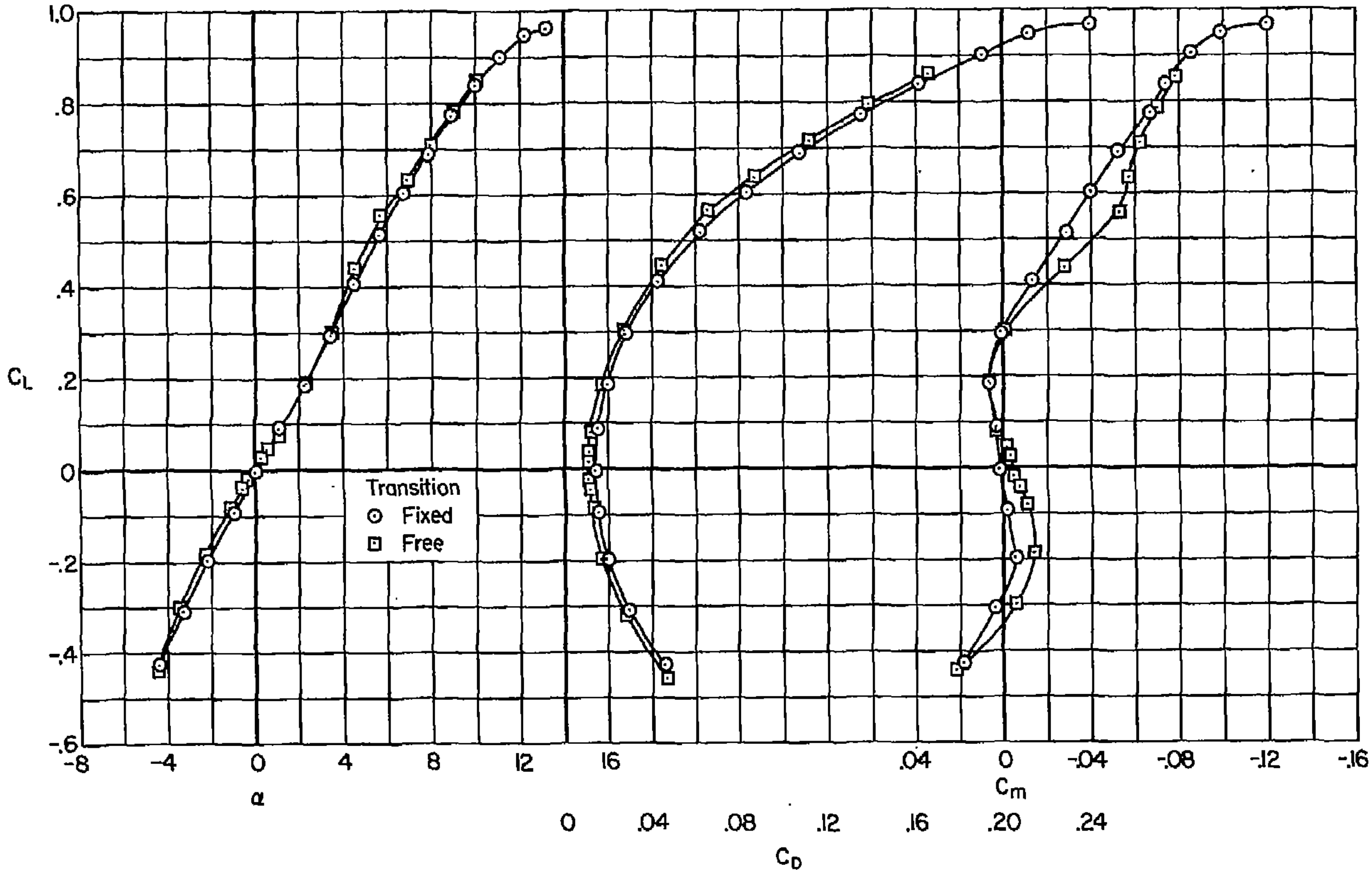

(b) Tail off, M = 0.94.

Figure 5.- Continued.

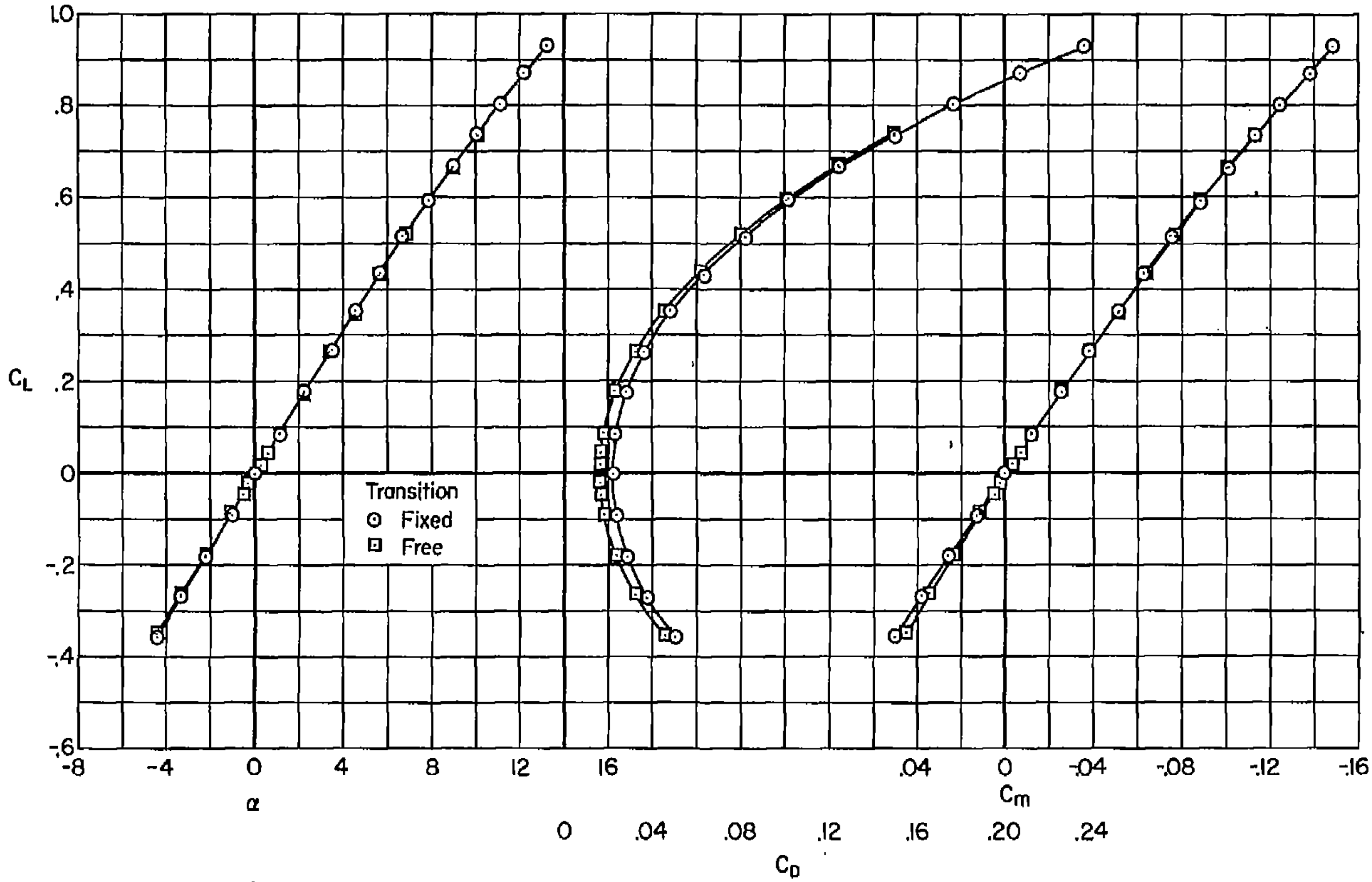

(c) Tail off, M = 1.20.

Figure 5.- Continued.

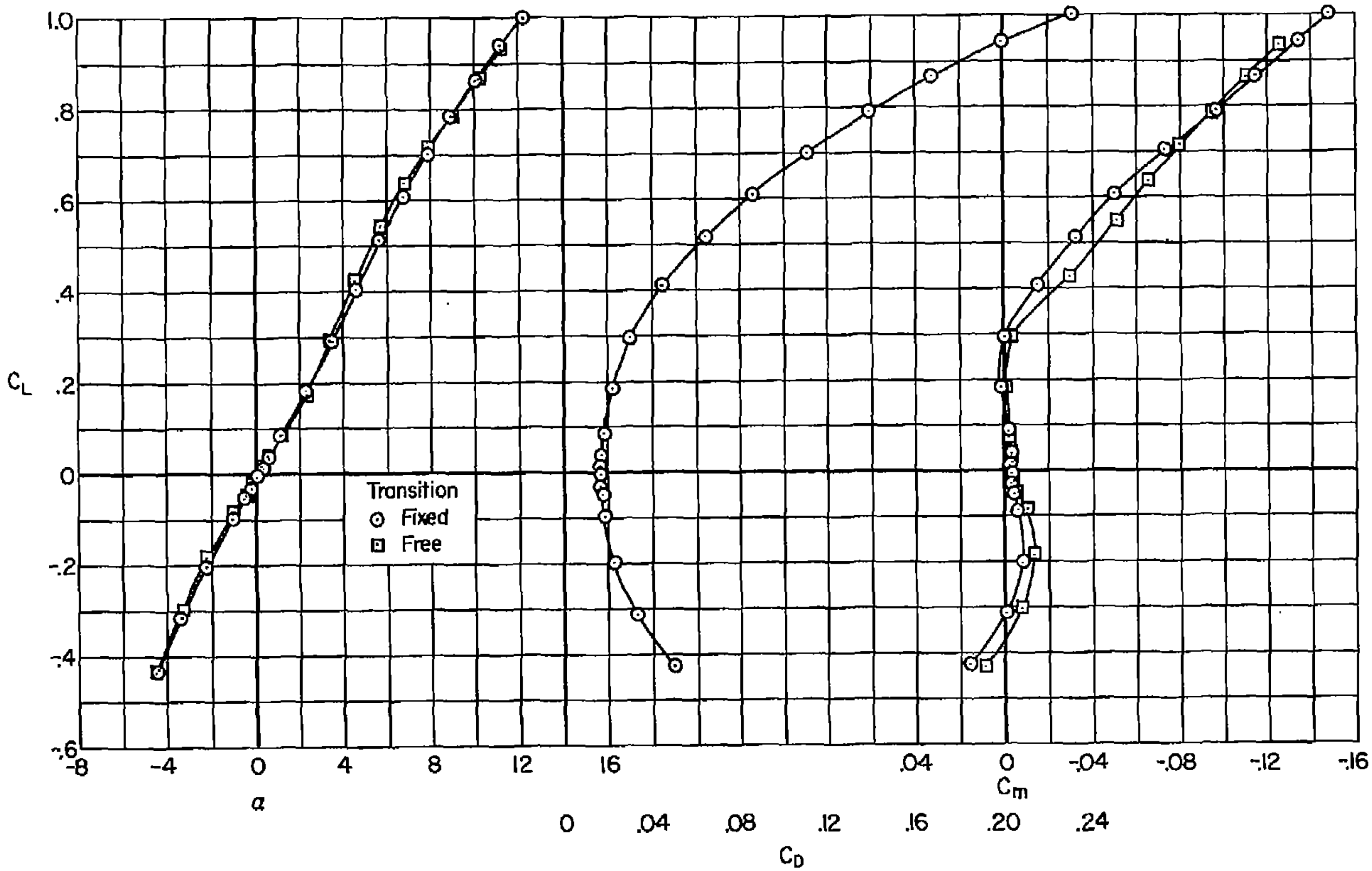

(a) Tail on, M = 0.94.

Figure 5.- Concluded.

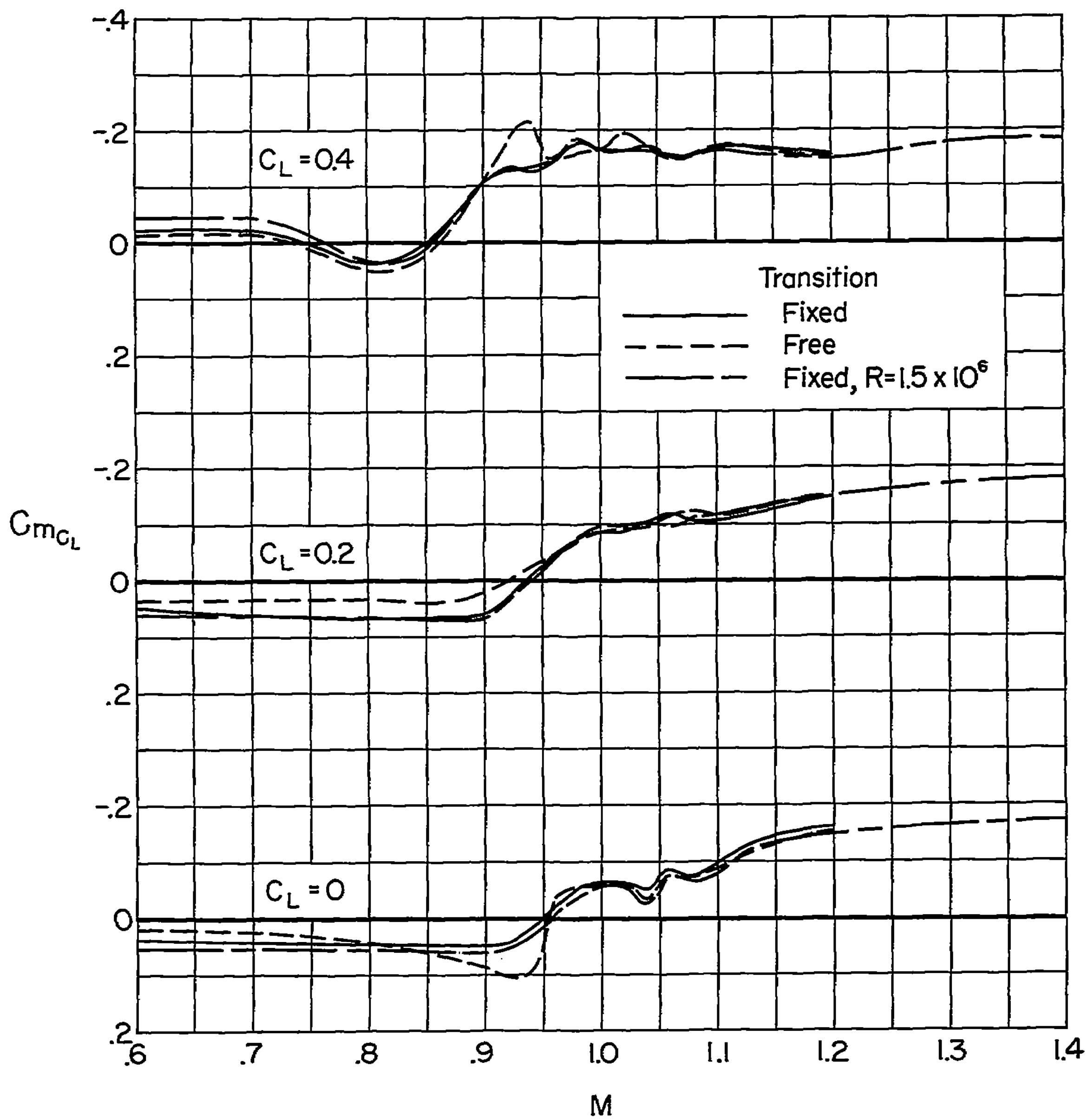

(a) R = 2.3×10[6], medium model.

Figure 6.- Variations of pitching-moment curve slope with Mach number for Reynolds numbers higher than 1.5×10[6] as affected by fixing transition; tail off.

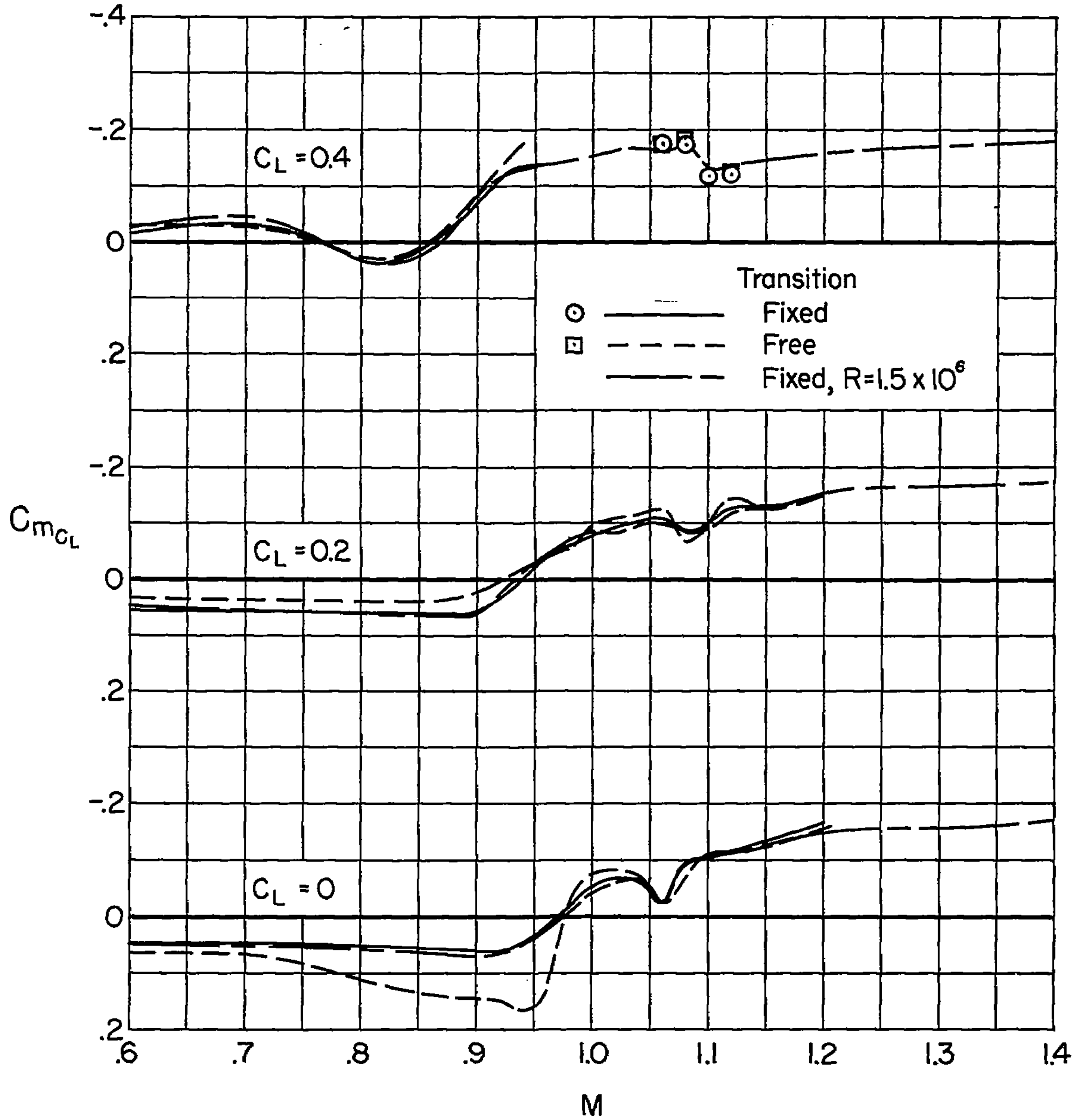

(b) $R = 3.45 \times 10^6$, large model.

Figure 6.- Concluded.

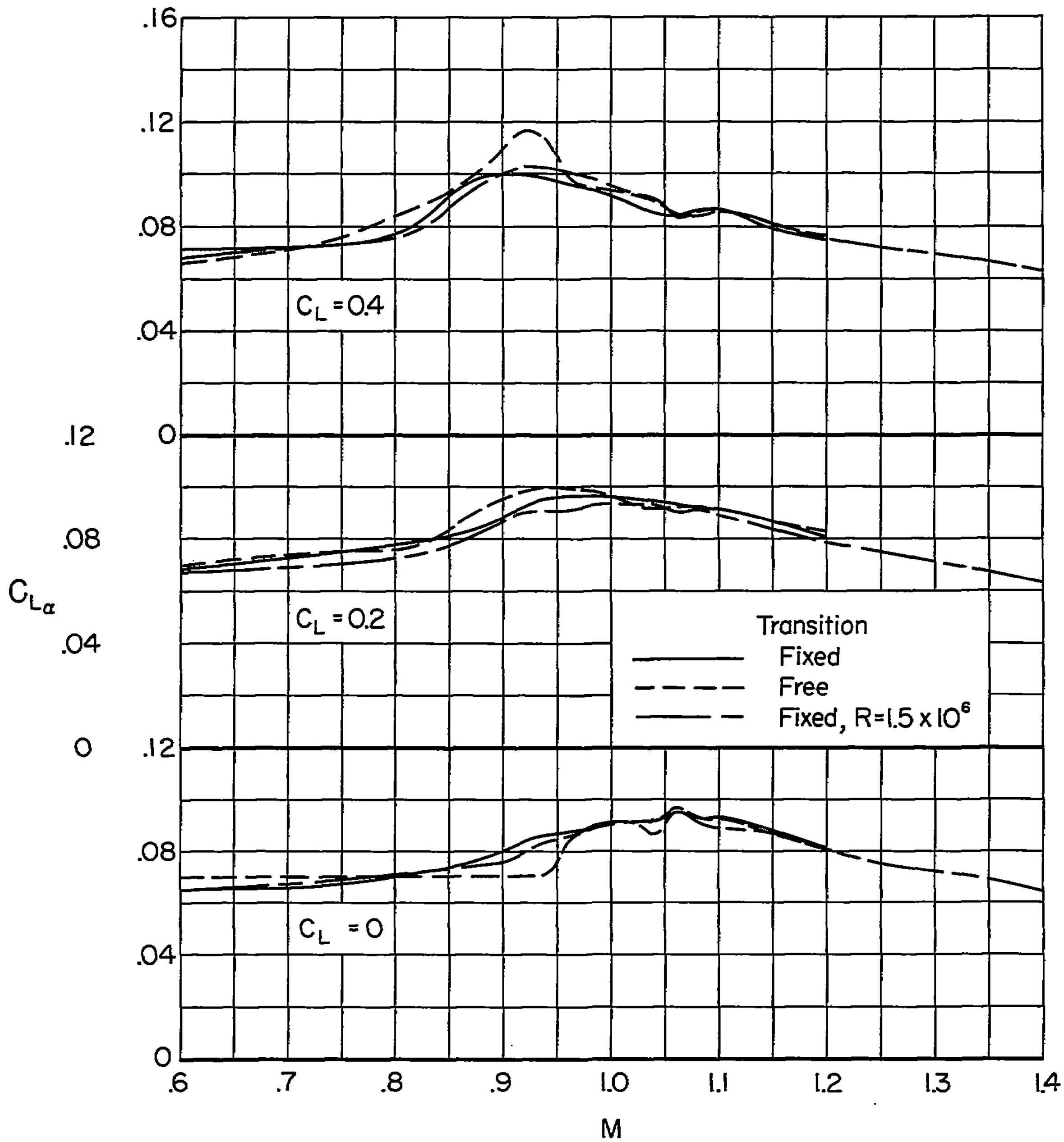

(a) R = 2.3×10[6], medium model.

Figure 7.- Variations of lift curve slope with Mach number for Reynolds numbers higher than 1.5×10[6] as affected by fixing transition; tail off.

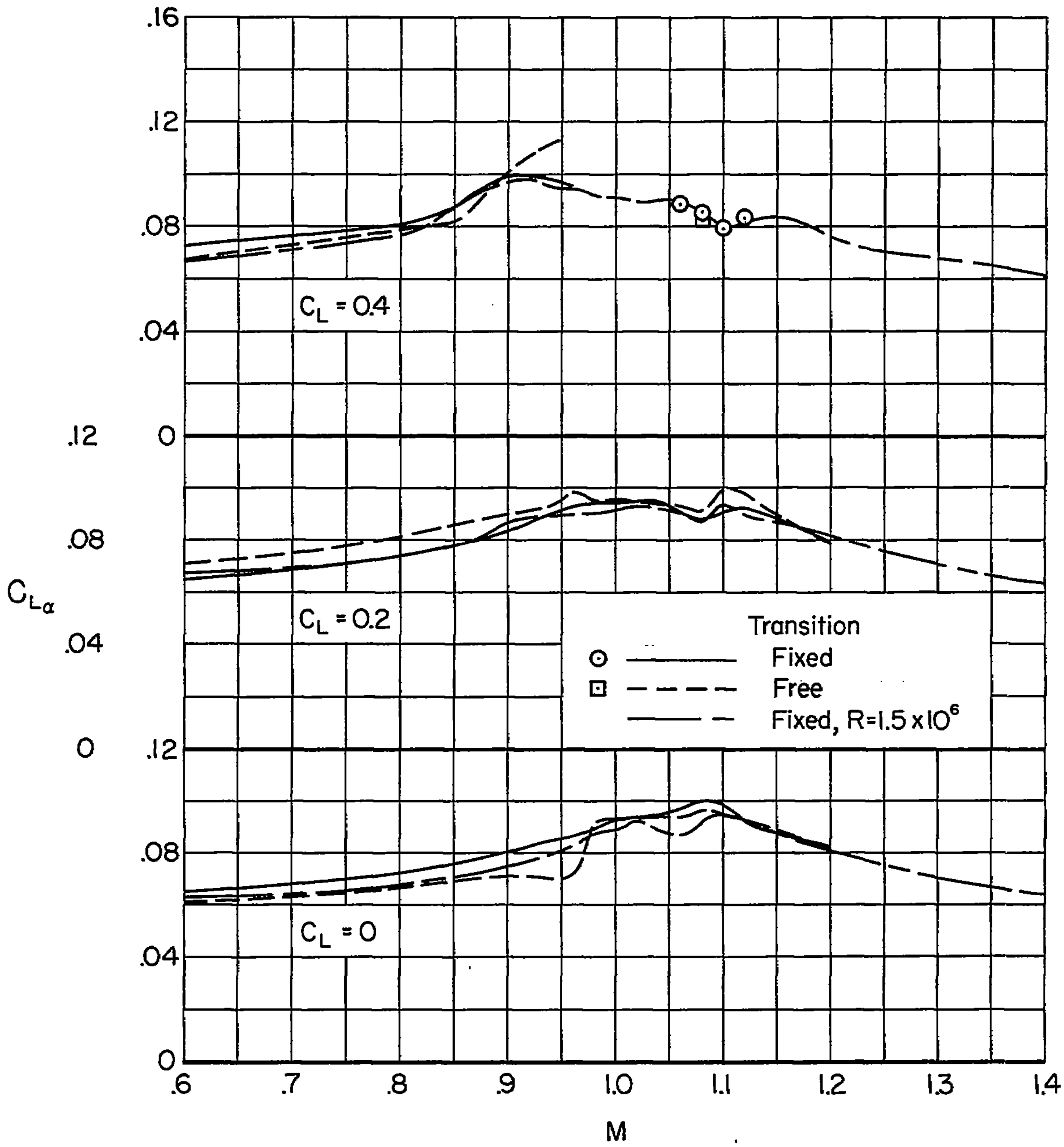

(b) R = 3.45×10[6], large model.

Figure 7.- Concluded.

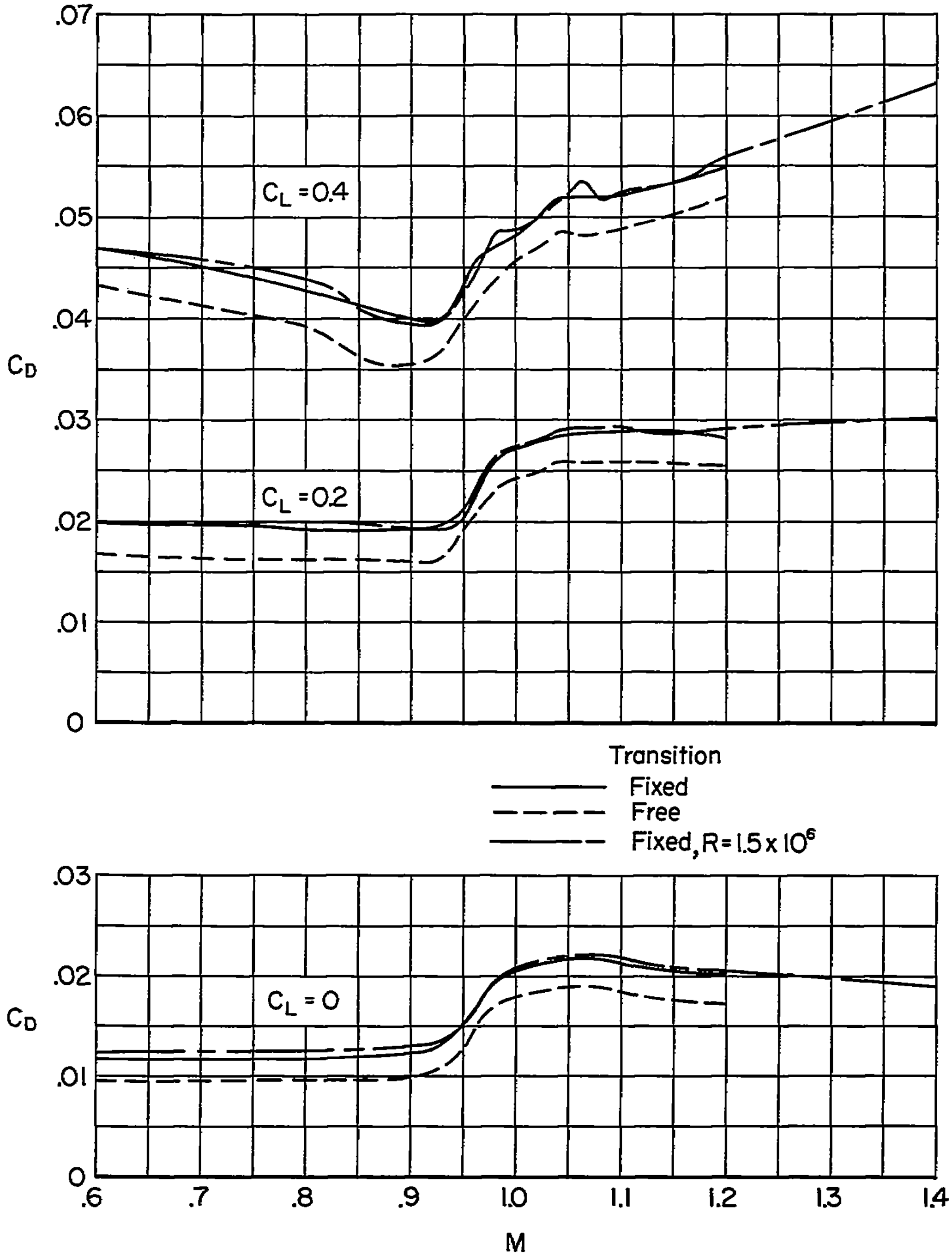

(a) $R = 2.3 \times 10^6$, medium model.

Figure 8.- Variations of drag coefficient with Mach number for Reynolds numbers higher than 1.5×10^6 as affected by fixing transition; tail off.

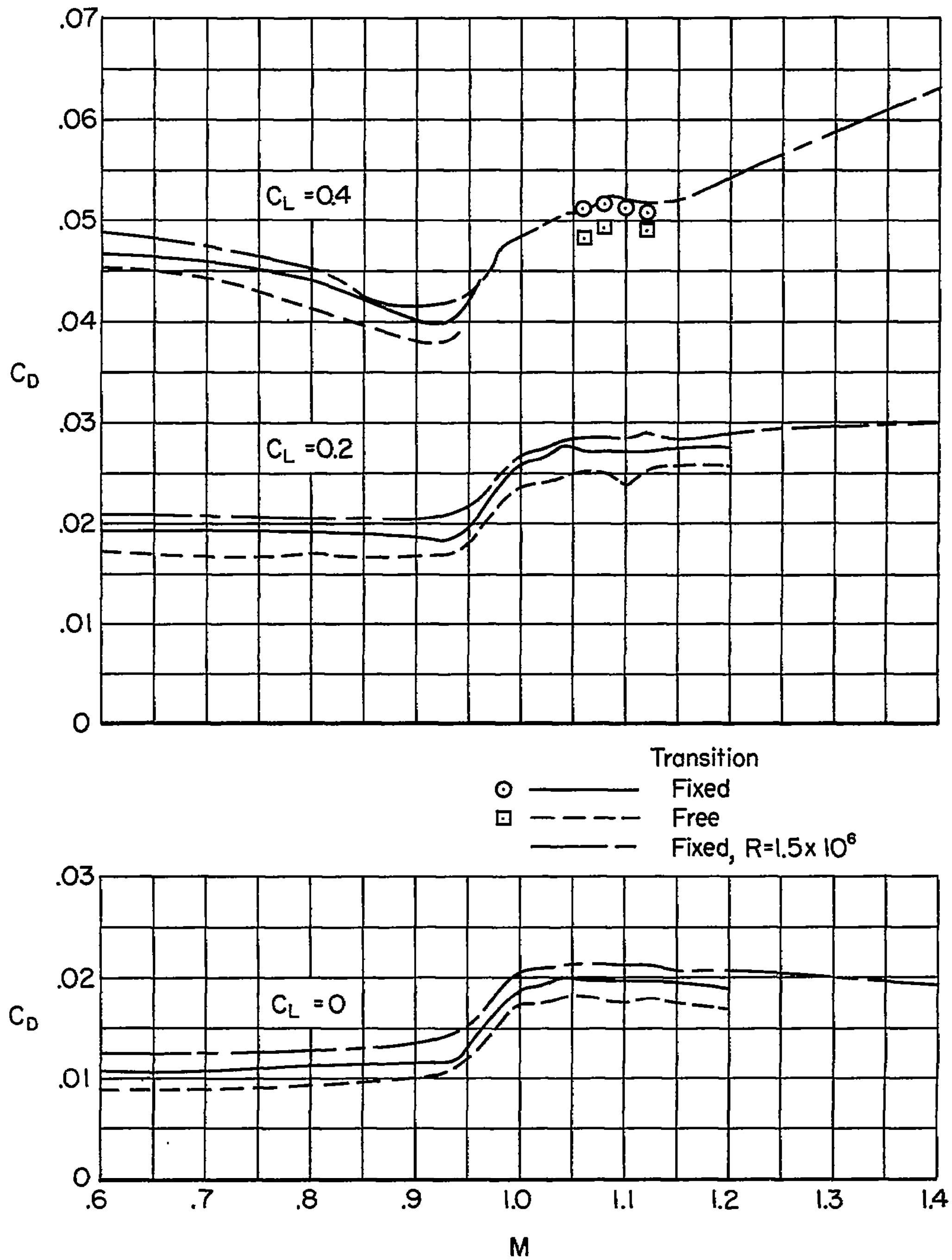

(b) R = 3.45×10[6], large model.

Figure 8.- Concluded.

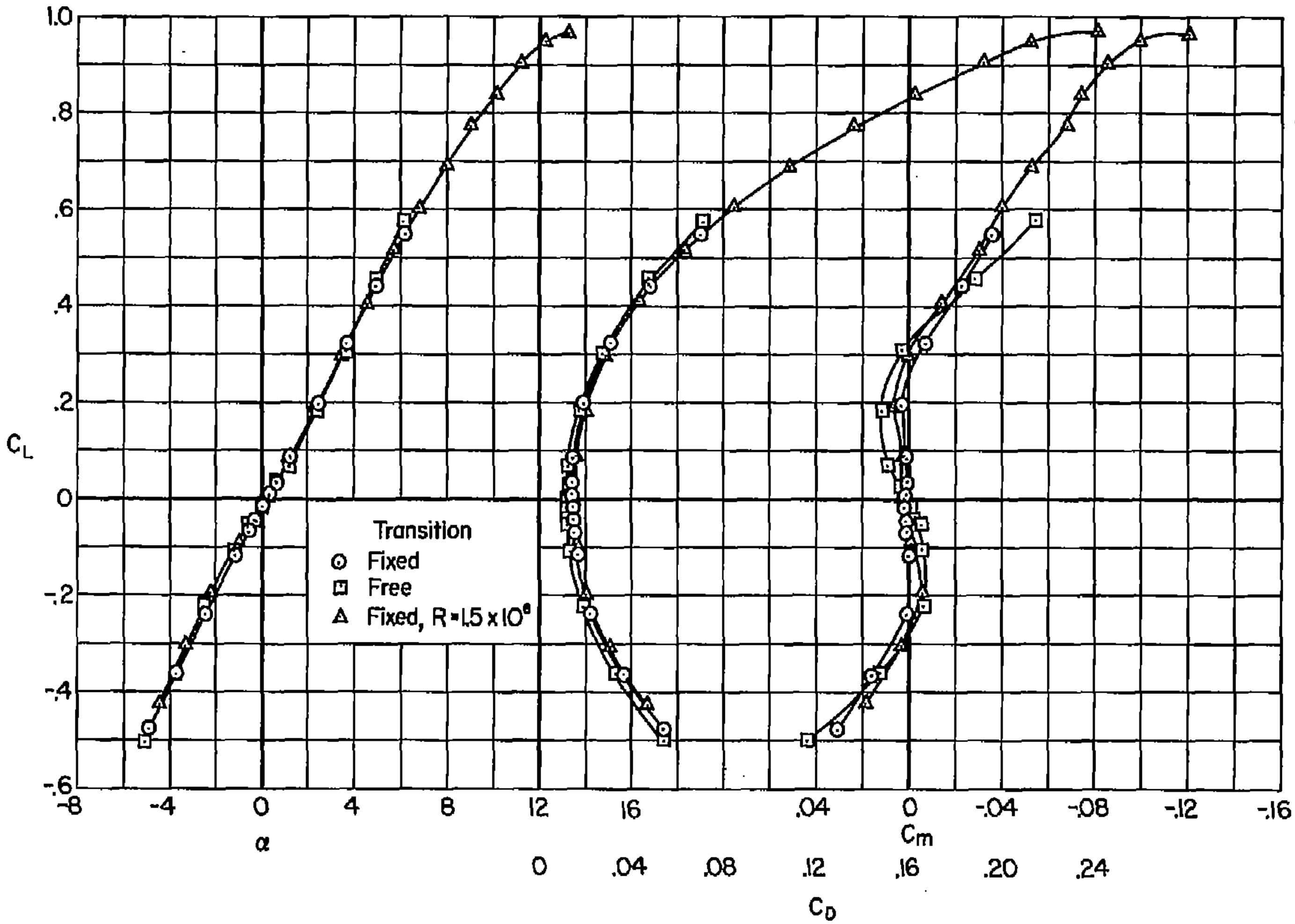

(a) $R = 2.3 \times 10^6$, medium model.

Figure 9.- Lift, drag, and pitching-moment characteristics for Reynolds numbers higher than 1.5×10^6 as affected by fixing transition; M = 0.94, tail off.

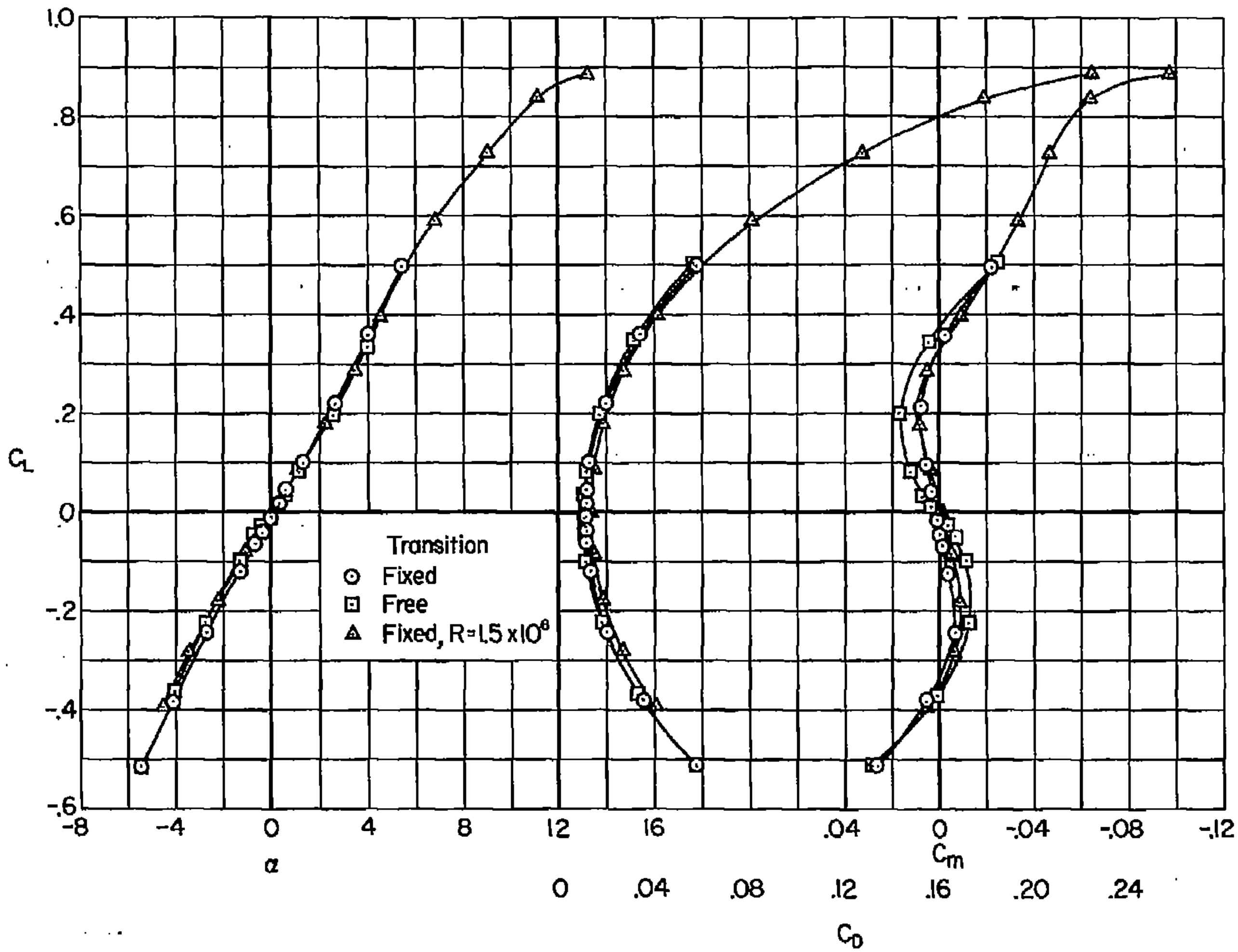

(b) $R = 3.45 \times 10^6$, large model.

Figure 9.- Concluded.

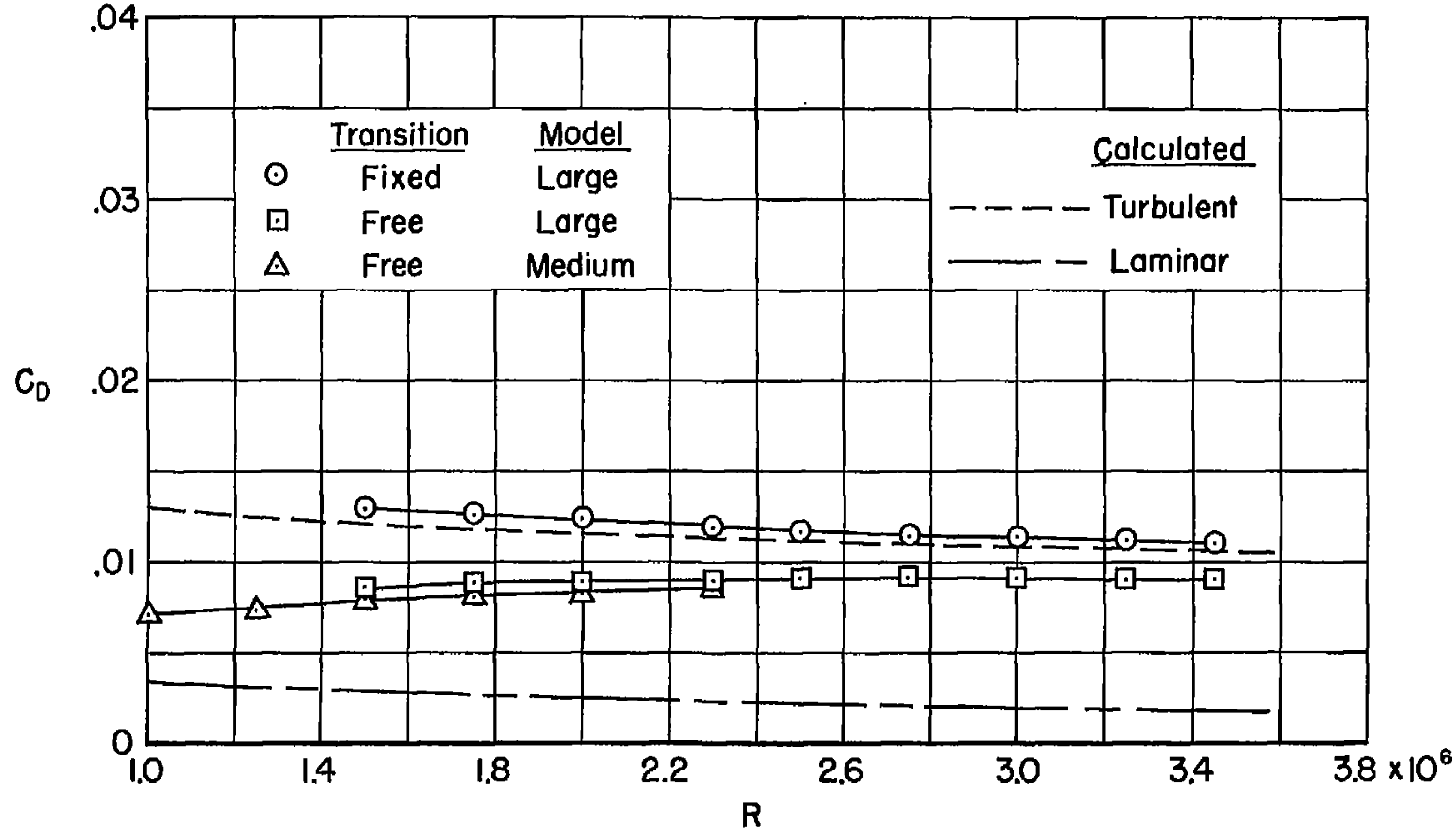

Figure 10.- Variations of drag coefficient with Reynolds number as affected by fixing transition; $C_L = 0$, $M = 0.60$, tail off.

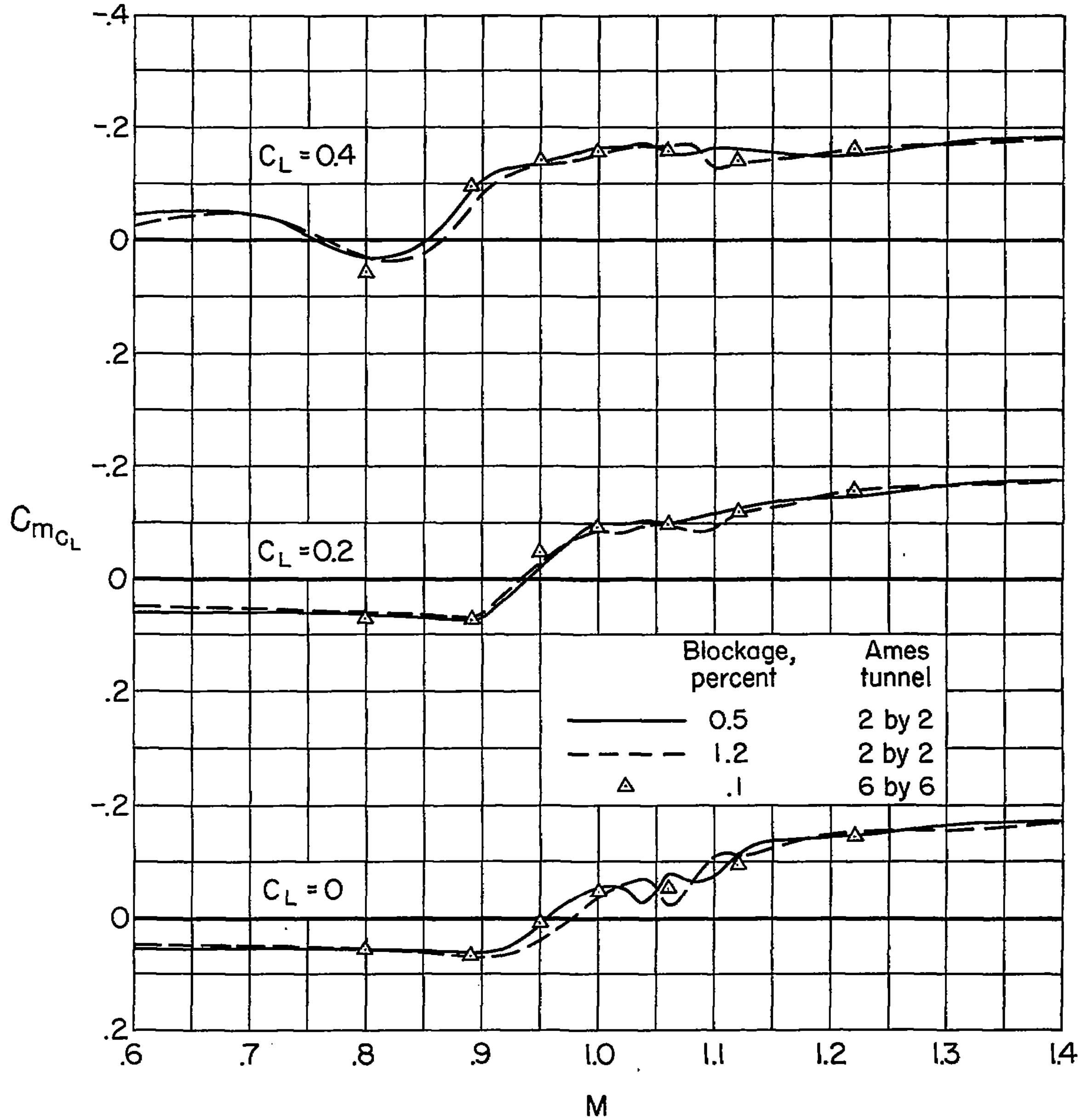

Figure 11.- Variation of pitching-moment curve slope with Mach number as influenced by the magnitude of model blockage; tail off, transition fixed, $R = 1.5 \times 10^6$.

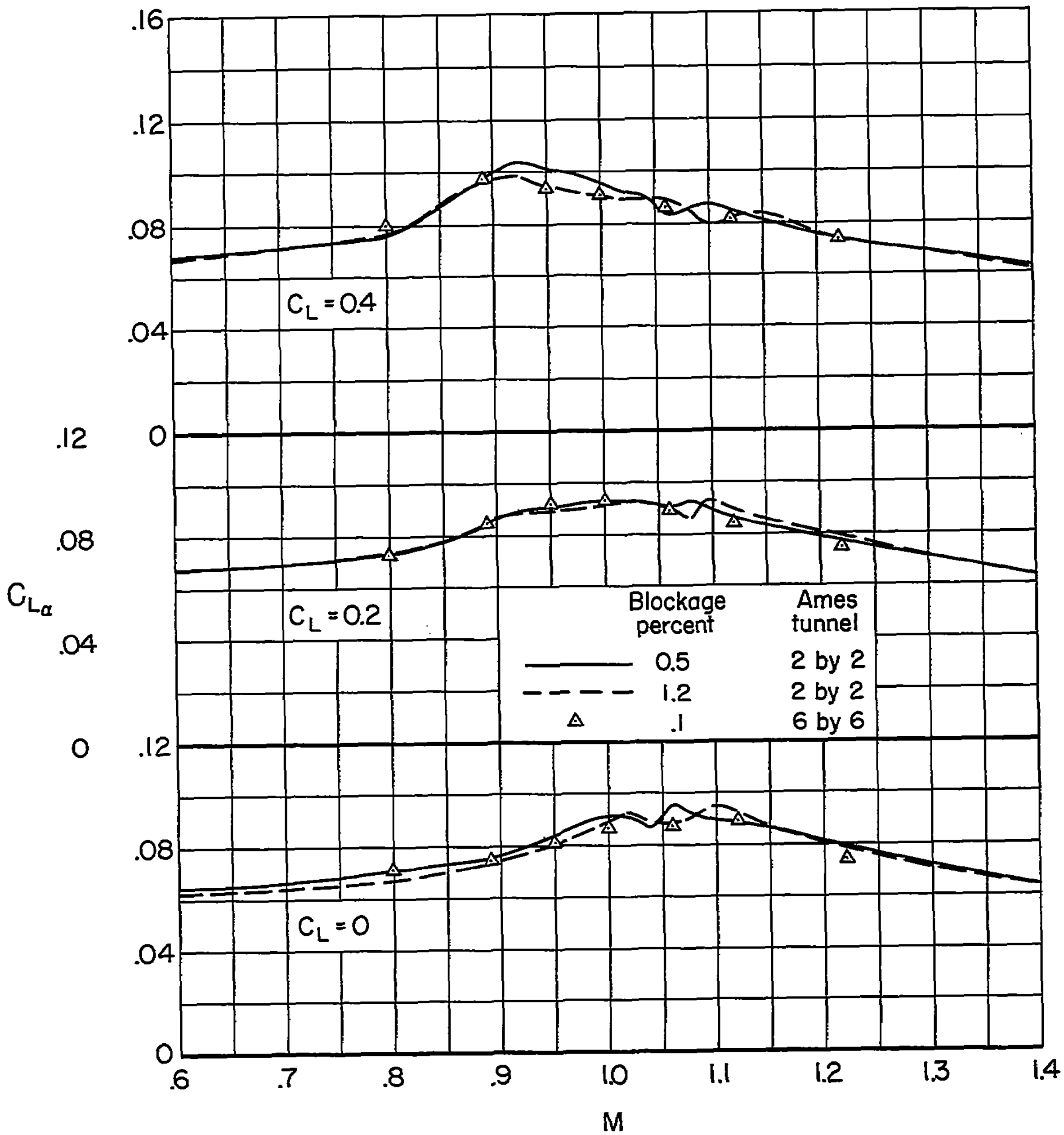

Figure 12.- Variation of lift curve slope with Mach number as influenced by the magnitude of model blockage; tail off, transition fixed, $R = 1.5 \times 10^6$.

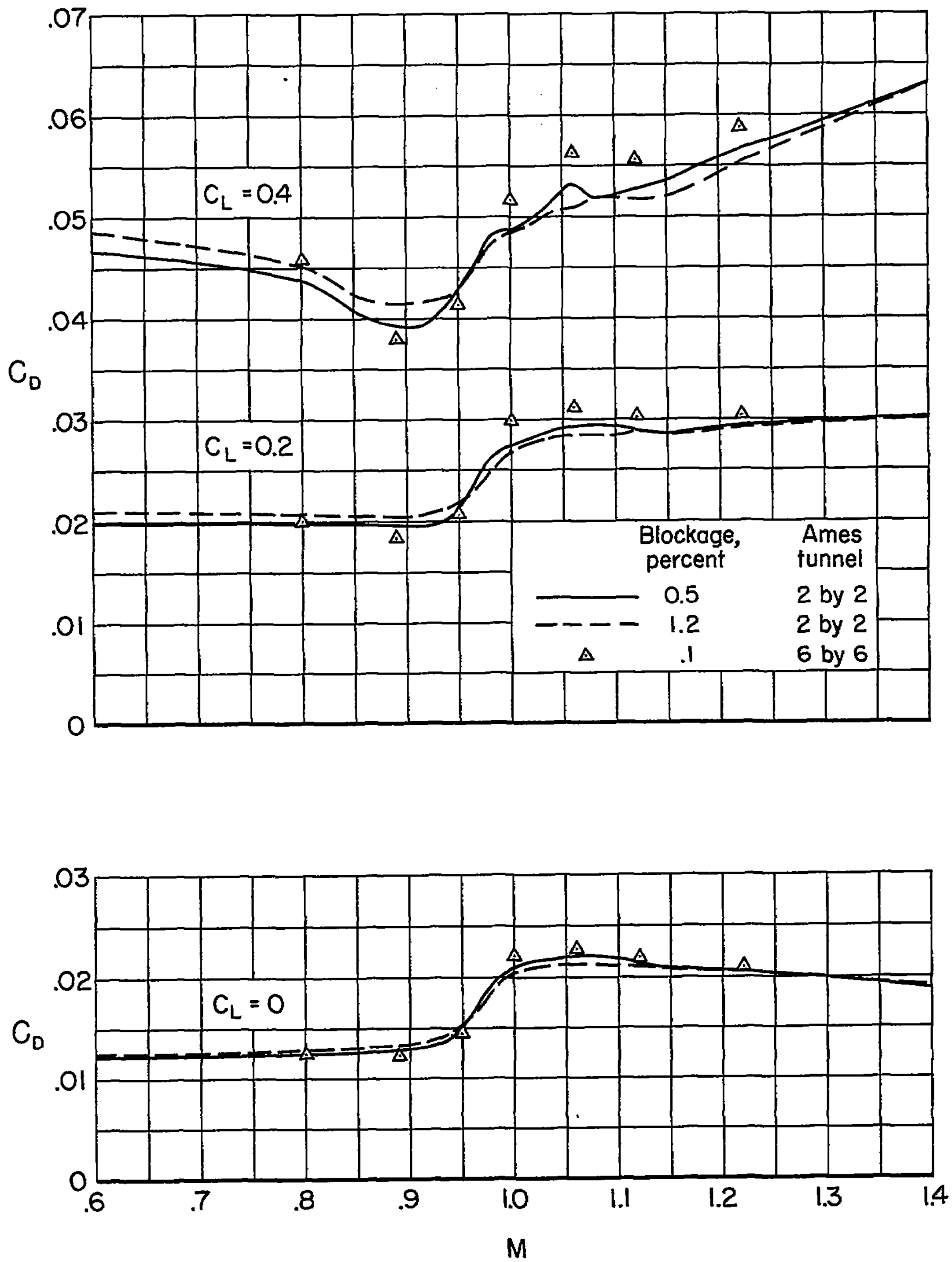

Figure 13.- Variation of drag coefficient with Mach number as influenced by the magnitude of model blockage; tail off, transition fixed, $R = 1.5 \times 10^6$.

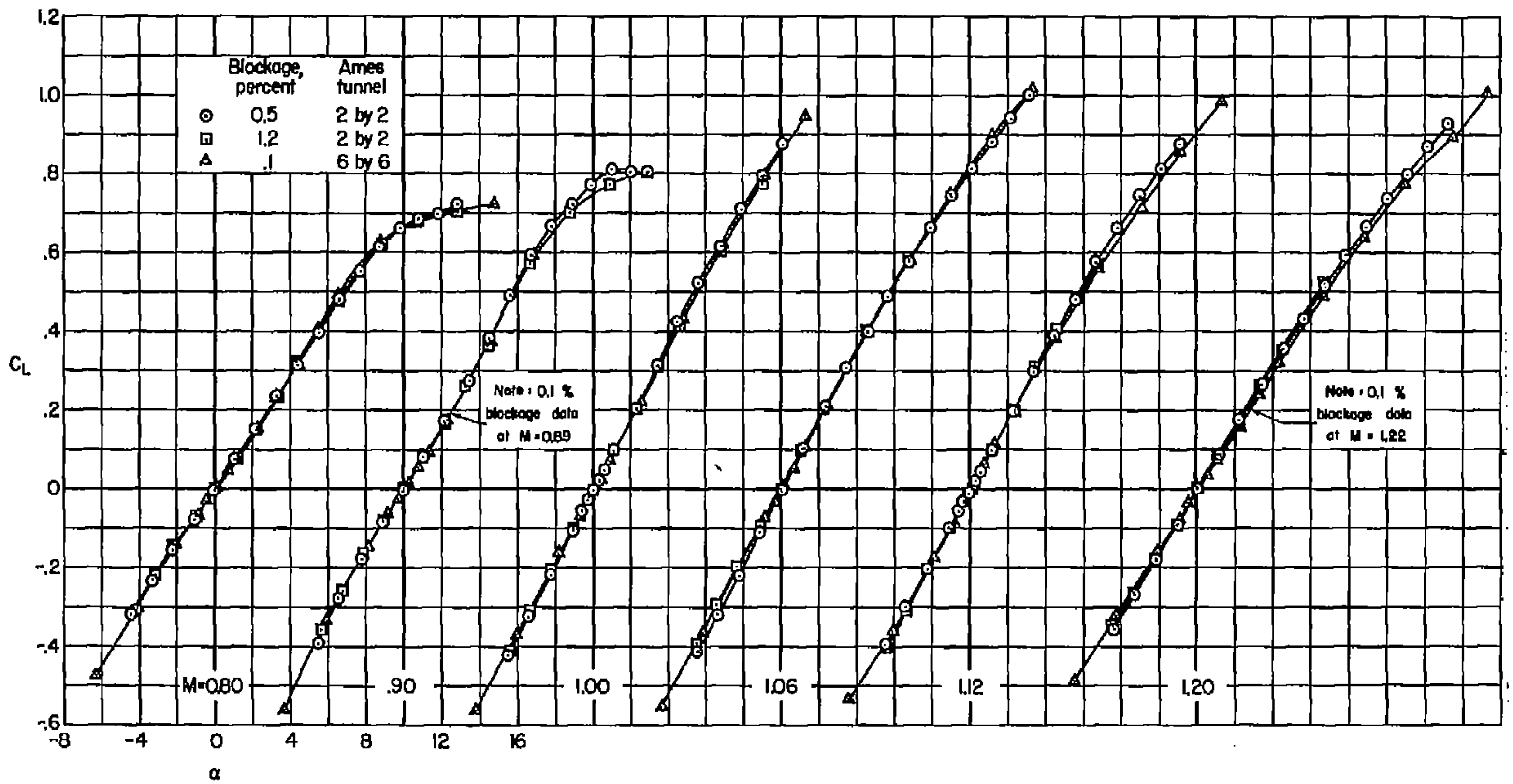

(a) C_L vs. α

Figure 14.- Lift, drag, and pitching-moment characteristics as influenced by the magnitude of model blockage; tail off, transition fixed, $R = 1.5 \times 10^6$.

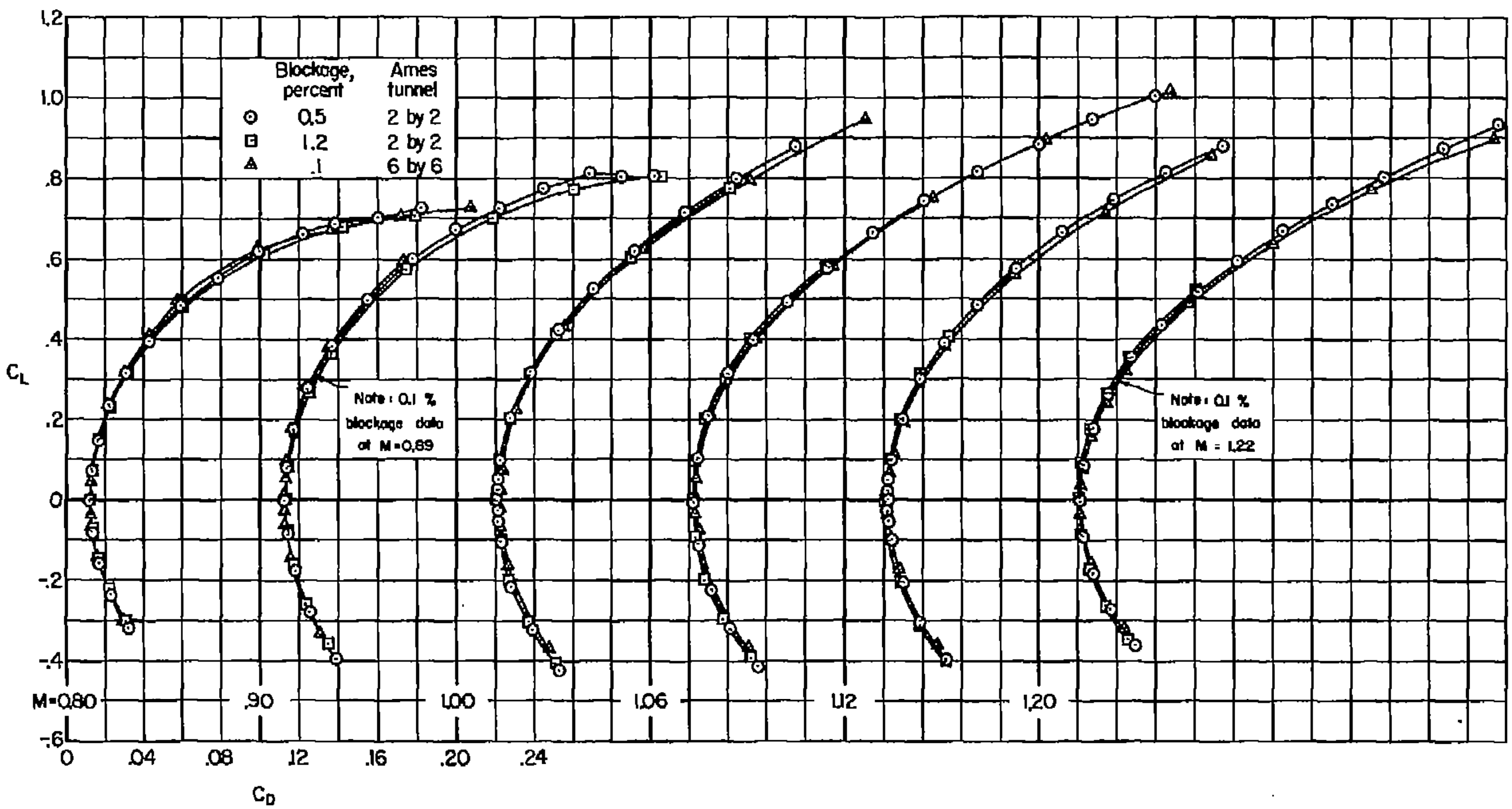

(b) C_D vs. C_L

Figure 14.- Continued.

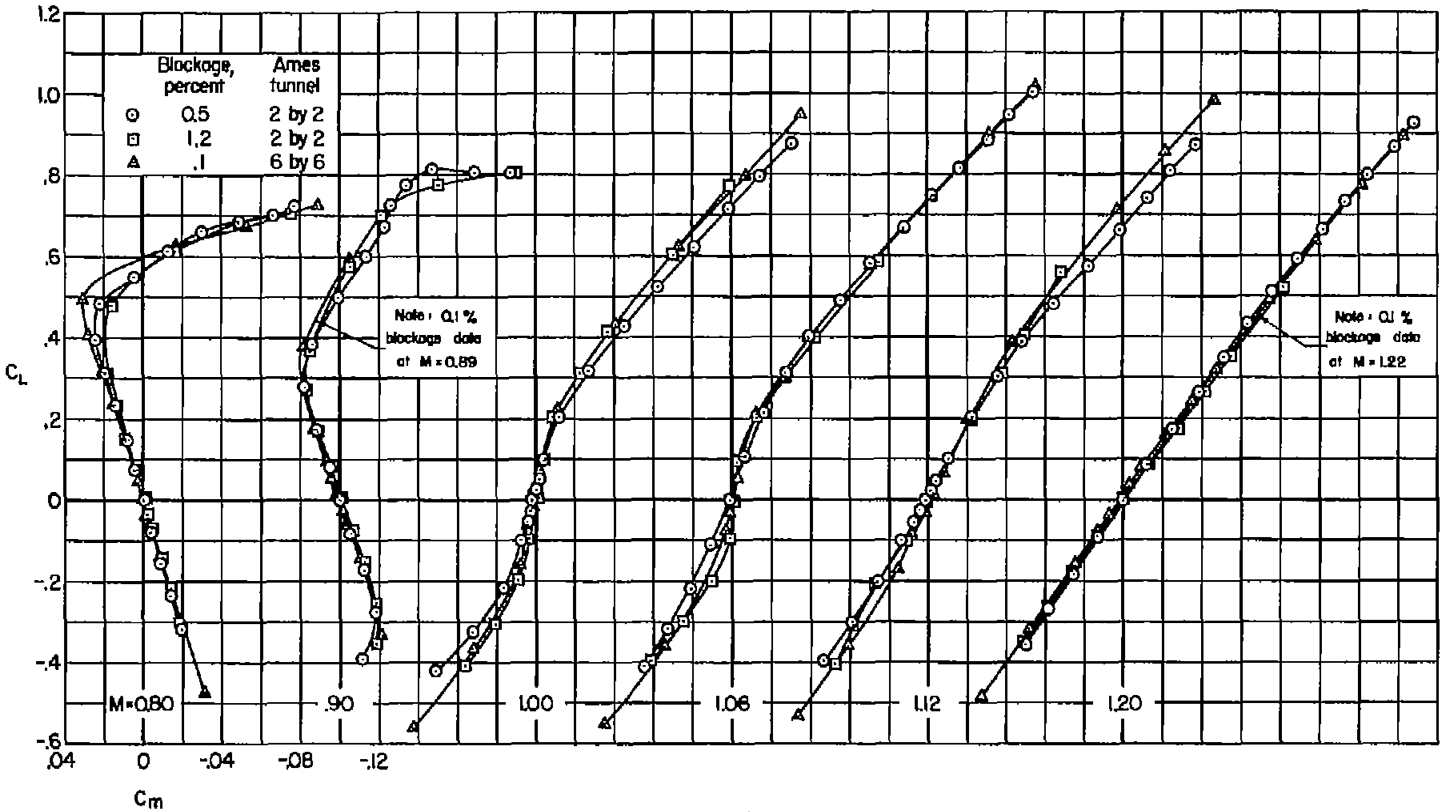

(c) C_m vs. C_L

Figure 14.- Concluded.